Food Hydrocolloids 124 (2022) 107301

Contents lists available at ScienceDirect

Food Hydrocolloids

journal homepage: www.elsevier.com/locate/foodhyd

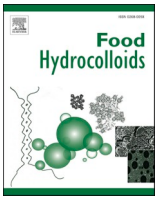

Engineering amyloid and amyloid-like morphologies of β-lactoglobulin

L.J.G. Hoppenreijs [a], L. Fitzner [b], T. Ruhmlieb [b], T.R. Heyn [b], K. Schild [a,b], A.-J. van der Goot [a], R. M. Boom [a], A. Steffen-Heins [b], K. Schwarz [b], J.K. Keppler [a,b,*]

[a] Laboratory of Food Process Engineering, Wageningen University & Research, Bornse Weilanden 9, 6708 WG, Wageningen, the Netherlands
[b] Division of Food Technology, Kiel University, Heinrich-Hecht Platz 10, 24118, Kiel, Germany

ARTICLE INFO

Keywords:
Aggregation
Flexibility
Fibrils
Worm-like aggregates
Peptides
Network

ABSTRACT

Background: Depending on environmental conditions, almost all proteins can form amyloid and amyloid-like aggregates that have unique functional properties. This opens numerous applications for designed aggregates in materials, medical and food applications. However, it is poorly understood how the amyloid (-like) aggregation and their resulting morphology is induced or influenced by various environmental and processing conditions.

Scope and approach: We identified and summarized conditions under which amyloid (-like) aggregates are formed and their impact on aggregate morphology. The focus is on β-lactoglobulin, but generic effects on other proteins are discussed, in order to elucidate common mechanistic properties.

Key findings and conclusions: The flexibility of linear aggregates can be evaluated by comparing the persistence (L_p) and contour length (i.e., length when completely stretched; L_c). Shorter and more flexible amyloid-like aggregates ($L_p < L_c$) usually occur from a relatively fast assembly (e.g., low repulsion, high concentration, solvents). Longer, semi-flexible amyloid aggregates ($L_p \sim L_c$) based on fibrillization-prone peptides that are slowly formed and assembled (e.g., high repulsion, low concentration). In either case, the aggregation kinetics increases through protein destabilization (e.g., heating, zinc addition, solvent and hydrolysis effects) and decreases through stabilization (e.g., glycerol addition). Post-processing (e.g., mechanical or interfacial stress) fragments aggregates into stiffer rods ($L_p > L_c$). Semi-flexible morphologies can align in liquid crystalline phases or interact with linear polysaccharides; while flexible aggregates can entangle. This allows for various possibilities to build higher order fibril or hybrid networks for various applications, such as bundles, coatings/films, or gels.
This knowledge is crucial to produce specific morphologies for applications and to draw conclusions about how morphologies will be affected during processing (e.g., shearing).

1. Introduction

Amyloid aggregation is a type of protein aggregation in which linear self-assemblies are formed through intermolecular stacking of β-sheets under specific circumstances. Amyloids have been mostly associated with neurodegenerative diseases, but it is increasingly accepted that all proteins can form amyloid structures, including food proteins (Cao & Mezzenga, 2019), and do this to some extend during food preparation, e.g. during boiling of egg white (Monge-Morera et al., 2020).

Amyloid structures with specialized functions are also evident in various organisms ranging from bacteria to mammals. For example, functional amyloids are involved in the attachment of mussels (Priemel, Degtyar, Dean, & Harrington, 2017) and squids (Deepankumar et al., 2020) to foreign surfaces, and in the colonization of bacteria and yeast (Fowler, Koulov, Balch, & Kelly, 2007), which illustrates their high (wet-resistant) surface adhesive properties. Additionally, they mechanically stabilize shells of insects and fish eggs, revealing their strong structural properties (Fowler et al., 2007). In plant seeds, amyloid-like aggregates stabilize storage proteins through their high stability, resistance to proteolysis and toxicity against fungal and mammalian cells

Abbreviations: AGE, advanced glycation end-product; β2m, β2-microglobulin; BLG, β-Lactoglobulin; BSA, bovine serum albumin; CMC, critical micelle concentration; DMSO, Dimethyl sulfoxide; DTT, dithiothreitol; EGCG, epigallocatechin-3-gallate; L_c, contour length; L_p, persistence length; RCM-BLG, reduced and carboxymethylated BLG; SDS, Sodium dodecyl sulphate; TEM, transmission electron microscopy; ThT, Thioflavin-T; WPC, whey protein concentrate; WPI, whey protein isolate.

* Corresponding author. P.O. Box 17, 6700 AA, Wageningen, the Netherlands
E-mail address: julia.keppler@wur.nl (J.K. Keppler).

https://doi.org/10.1016/j.foodhyd.2021.107301
Received 27 May 2021; Received in revised form 21 October 2021; Accepted 21 October 2021
Available online 25 October 2021
0268-005X/© 2021 The Authors. Published by Elsevier Ltd. This is an open access article under the CC BY license (http://creativecommons.org/licenses/by/4.0/).

(Antonets et al., 2020). Although there is an ongoing debate around the safety of engineered aggregates that needs to be resolved before any applications can be produced for human consumption, the outstanding properties of amyloid structures in nature is an inspiration for engineered functional amyloid aggregates from (food) proteins. Bovine β-lactoglobulin (BLG) is the most abundant protein in whey and is extensively studied and used in the food industry. Amyloid aggregates of BLG or whey protein isolate (WPI) are reported to be, for example, efficient gelators (at 0.3 wt%; Veerman, Baptist, Sagis, & Van der Linden, 2003), emulsifiers (Cao & Mezzenga, 2019), encapsulates (Humblet-Hua, Van Der Linden, & Sagis, 2012), and are good carriers for iron (Shen et al., 2017) and curcumin (Mohammadian et al., 2019). In addition, films from BLG amyloid aggregates are remarkably strong, having a comparable elastic modulus to keratin and collagen (Knowles, Oppenheim, Buell, Chirgadze, & Welland, 2010). Many novel materials from BLG amyloid aggregates have already been described, which could be used e.g., as biosensors, nanocomposites, or catalysts (Wei et al., 2017).

The functionality of amyloid aggregates is in particular attributed to their specific high aspect ratio (i.e., length/thickness; Knowles & Mezzenga, 2016). Besides the classical straight amyloids, BLG can form 'amyloid-like' aggregates when the β-sheets are less tightly stacked, which are shorter and more flexible. The linear BLG aggregate morphology therefore varies from short, single-stranded, worm-like and flexible aggregates to long, multi-stranded, straight and semi-flexible fibrils (Jordens, Adamcik, Amar-Yuli, & Mezzenga, 2011). Semi-flexible fibrils with a high aspect ratio, effectively increase the viscosity and form gels. Worm-like aggregates increase the viscosity much less, at comparable concentrations (Loveday, Anema, & Singh, 2017). Amyloid aggregates display effective emulsifier properties through a Pickering mechanism, protecting droplets from coalescence. The binding is particularly strong for anisotropic particles. For example, in the case of fibrils, it is practically impossible to detach them once they have attached to a surface (Jordens, Isa, Usov, & Mezzenga, 2013). Therefore, several morphologies with varying application potential can be produced, by adapting environmental and processing conditions.

Conditions at which BLG forms amyloid (-like) structures are high concentrations of urea (Hamada & Dobson, 2009), alcohols (Gosal, Clark, & Ross-Murphy, 2004), or at a combination of elevated temperature, low pH, and low ionic strength (Heyn et al., 2020). These conditions initially destabilize the native protein and form the aggregate building blocks: partly unfolded BLG and/or its constituent peptides. During the nucleation phase, the building blocks self-assemble into weakly associated nuclei. Further addition of building blocks during the growth phase results in the formation of linear aggregates. For insulin, it has been shown that the growth is unidirectional (Heldt, Zhang, & Belfort, 2011). Based on the role of specific conditions on the aggregation process, the conditions can be divided into aggregation and post-aggregation factors. Aggregation factors mainly include conditions or modifications that can affect the aggregate morphology through their impact on the balance between intra- and intermolecular interactions. Besides, the aggregation kinetics are influenced by all factors that result in a local increase of protein-protein collisions (e.g., shearing or surfaces). Post-aggregation factors affect and change the mature aggregate morphology, which includes the gradual modification of the properties, and fragmentation. For post-processing, the aggregate stability is important, which is determined by the internal molecular packing density of the aggregates and which is reflected in its morphology. In addition to the targeted post-processing of amyloid structures, fragmentation can occur unintendedly during food processing or storage. The final aggregate morphology and flexibility then determines the further assembly into higher order networks of bundles (one dimensional), at interfaces (two dimensional), or in gels (three dimensional), which then lead to various applications. Fig. 1 describes the major steps in the formation of protein aggregates.

Currently, an in-depth review on how to use physical and chemical conditions to modify BLG and subsequently tune the aggregate morphology and its assembly into multidimensional structures is lacking. Therefore, this review will discuss the conditions that favor the engineering of specific amyloid morphologies and will identify gaps in our knowledge. In addition, post-aggregation factors will be discussed, which are also relevant for further modification of the morphology, unintended or intended. We will not focus on the use amyloid structures for further applications, as this has already been reported earlier (Cao & Mezzenga, 2019; Jansens et al., 2019; Lambrecht et al., 2019; Loveday et al., 2017).

We will first summarize the primary conditions that affect the aggregate morphology, namely the pH, ionic strength, temperature and protein concentration. We will then discuss the effects of the physical processing conditions, such as shearing, cavitation and pressure, that mainly affect the fragmentation of mature amyloid structures. Also, the influence of the presence of solid/liquid and liquid/liquid interfaces will be discussed. Besides physical processing, the chemical environmental conditions can be adapted to modify the structure of proteins and subsequently the aggregation behavior. Finally, we will touch upon how the individual fibrils with specific morphology can associate into higher order networks, forming fibers, films and gels with high mechanical stability.

2. The primary conditions: pH value, ionic strength and temperature

Amyloid aggregates are formed through the formation of building blocks from the individual proteins and the subsequent assembly of these building blocks. The building blocks of amyloid aggregates are (partly) unfolded or hydrolyzed BLG, which contain (exposed) fibrillization-prone sequences. In particular, the factors and factor combinations of pH value, ionic strength, and temperature are of crucial

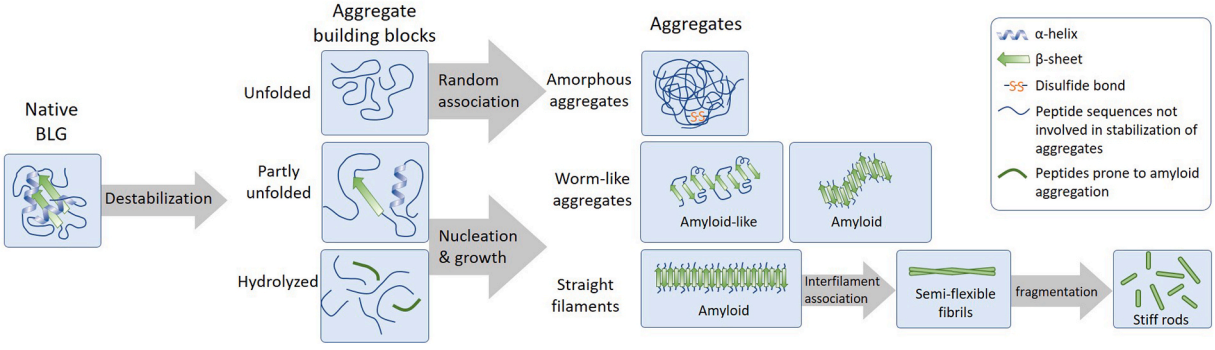

Fig. 1. Schematic overview of the general self-assembly of destabilized BLG into aggregate building blocks and subsequent aggregates with amorphous, worm-like or straight morphology.

importance for the exposure or formation of such fibrillization-prone building blocks, their aggregation kinetics, and the resulting aggregate morphology. In the following section, an overview of the conventional fibril formation conditions for BLG is given, starting with the effect of the pH value, the ionic strength and the temperature on the resulting morphologies (section 2.1), followed by the effect of these primary conditions to tune the morphology of mature fibrils (section 2.2.) and ending with an outlook on fibril morphology of other food proteins under these conditions (section 2.3).

2.1. Aggregation

The most common environmental conditions for the formation of different amyloid (-like) aggregates from BLG are low pH (≤3.5), low ionic strength and elevated temperature (>70 °C), resulting in typical semi-flexible fibrils. Random aggregation is prevented by the electrostatic repulsion induced through low pH values (≤3.5). At pH < 3, the association of intact BLG is unfavorable and hydrolysis is necessary to allow for amyloid aggregation. Acid hydrolysis within the relevant time frame (several hours) can be induced by heating at >70 °C (typically 80–90 °C), leading to the formation of peptides with increased fibrillization propensity. These peptides include mainly the N-terminal peptide sequences 1–33 and 1–53. The inclusion of these specific peptide sequences is mainly attributed to their increased hydrophobicity, capacity to form β-sheets and low charge (Akkermans et al., 2008). Specific amino acid residues can stabilize the intermolecular β-sheets. For example, through hydrogen bonds by amide-containing residues (glutamine and asparagine; Heyn, 2020) or π–π stacking of aromatic groups in aromatic residues (phenylalanine and tryptophan; Porat, Abramowitz, & Gazit, 2006).

Association of these fibrillization-prone peptides results in thin (~2.6 nm), long (contour length, L_c = 0.2–5 μm), straight and well-ordered amyloid aggregates (Fig. 2A; Akkermans et al., 2008; VandenAkker, Engel, Velikov, Bonn, & Koenderink, 2011). The flexibility of these aggregates can be evaluated by comparing the persistence (L_p) and contour length (axial circumference), which are of the same order of magnitude for less flexible structures. VandenAkker et al. (2011) showed that this is the case for the fibrils (L_p = 3.8±0.1 μm) and therefore we will refer to these structures as 'semi-flexible fibrils' (Fig. 2A). Besides, their folding density is approximately 2% higher as compared to native BLG (Uttinger et al., 2020). Since only a fraction of the total protein peptide chain is included in the fibrils, the maximum conversion factor for incorporation is only 40–50% (Bolder, Vasbinder, Sagis, & van der Linden, 2007; Serfert et al., 2014). BLG is the main constituent of WPI and makes up about half of the total protein content. WPI shows similar fibrillization kinetics and fibril morphology, since only BLG is incorporated in the fibrils at pH 2 and 80 °C. Further proteins present in WPI (α-lactalbumin and bovine serum albumin) are mostly inert to fibrillization under these conditions. However, they can form small aggregates that are able to lower the gelation concentration of BLG fibrils by introducing depletion forces (Bolder, Hendrickx, Sagis, & Van Der Linden, 2006).

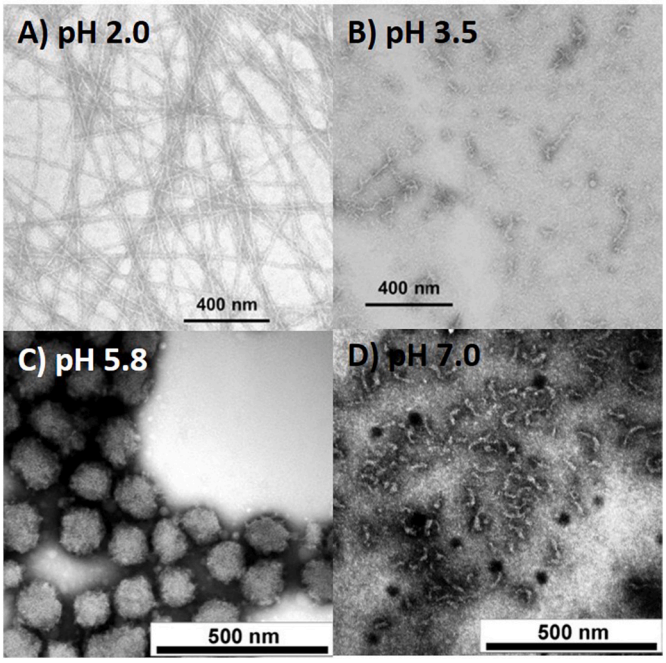

Fig. 2. TEM images of BLG aggregates prepared at (A) pH 2.0 and (B) pH 3.5 (both 2.5% BLG at 90 °C for 5 h, from Keppler et al. (2019), and (C) pH 5.8 and (D) pH 7.0 (both 1.0% BLG at 85 °C for 15 min, from Jung et al. (2008).

Besides semi-flexible fibrils, another type can be formed from BLG at higher pH values. At pH 3 to 3.5 and temperatures >70 °C (Heyn et al., 2020), partly unfolded BLG can directly associate into more randomly associated amyloid-like aggregates that are thin (1–3 nm) and short (L_c = 50–200 nm; Fig. 2B). We will refer to these structures as 'worm-like aggregates'. They are more flexible (L_p ~ 10 nm) than semi-flexible fibrils (Heyn et al., 2019; Jung, Savin, Pouzot, Schmitt, & Mezzenga, 2008). In addition, they are less compact, which is explained by the incorporation of unstructured (random coil) peptide sequences into the aggregates (Heyn et al., 2019). Lux et al. (2021) hypothesized that rearrangements for worm-like aggregates at pH 3.5 cause outward folding of the C-terminus. Ye, Hedenqvist, Langton, and Lendel (2018) demonstrated that a larger fraction of C-terminal peptides is included in the core segment of amyloid-like aggregates, due to the lower acid hydrolysis at higher pH value.

At pH values near the isoelectric point, the morphology shifts toward monodisperse, compact, and randomly associated spherical aggregates (~150 nm, Fig. 2C) (Jung et al., 2008). At neutral pH, which is generally somewhat higher than the isoelectric point, the electrostatic repulsion allows for aggregation into unbranched, short (<100 nm) and worm-like aggregates with a diameter of 6 ± 1 nm (Fig. 2D; Da Silva Pinto et al., 2012; Jung et al., 2008). The amyloid-like nature obtained by these authors was confirmed with a Thioflavin T (ThT) assay (Da Silva Pinto et al., 2012), which is frequently used as a first indicator of amyloid aggregation.

Enzymatic hydrolysis can be applied as an alternative to acid hydrolysis, to produce peptides with increased fibrillization propensity. Akkermans et al. (2008) reported that hydrolysis of BLG with the endoproteinase AspN allows for amyloid aggregation at a lower temperature (37 °C). After hydrolysis at pH 8 and a pH adjustment to pH 2, semi-flexible fibrils (~1 μm) and random aggregates (~50 nm) were formed. The obtained heterogeneity in the morphology was confirmed by Hamada et al. (2009), which shows that the morphology depends on the peptides that are involved in nucleation. Therefore, the type of proteinase determines whether fibril formation is enhanced or suppressed. For instance, Gao, Xu, Ju, and Zhao (2013) observed that the hydrolysis of whey protein concentrate (WPC) with trypsin allows fast fibril formation, while the hydrolysis with protease A, M and pepsin resulted in slower aggregation. Trypsin-treated WPC formed unbranched, long, semi-flexible fibrils, while WPC treated with the other enzymes resulted in shorter and/or branched fibrils after prolonged heating (5–10 h). The difference was mainly attributed to the ability of trypsin to preserve the α-helix structure, while the other enzymes destroyed 51–37% of this structure, which is transferred to β-strands and subsequent intermolecular β-sheets during fibrillization. Besides, they observed a decreased sulfhydryl group content during the hydrolysis for all enzymes, except trypsin, which indicated that additional disulphide bonds were formed. Intermolecular disulphide bond formation is expected to hinder amyloid aggregation. Lastly, aggregation was also stimulated by cleavage at hydrophobic amino acids as performed by trypsin, which lead to higher surface hydrophobicity of the resulting

peptides, as compared to cleavage by the other enzymes.

The initial protein concentration influences the amyloid morphology mainly through its impact on the size distribution of the peptides that result from acid hydrolysis. During acid hydrolysis, a gradual increase from pH 2 to pH 3 is observed, which then limits further hydrolysis and stimulate aggregation (Ye et al., 2018). This will occur faster at higher protein concentrations, and larger peptides are included in the aggregates. Low initial BLG concentrations are generally used (up to 3.0–4.0%, w/w), which results in semi-flexible fibrils. Higher concentrations (~7.5–8.0%, w/w) result in shorter and worm-like aggregates (L_c = 100–500 nm, L_p ~ 90 nm) with a similar diameter (~2.6 nm) (VandenAkker et al., 2011, 2016; Ye et al., 2018). These worm-like aggregates include more random coil and α-helix structures, while the semi-flexible fibrils contain more β-sheets (VandenAkker et al., 2016; Ye et al., 2018). Ye et al. (2018) attribute the differences in secondary structure to more incorporation of C-terminal peptides, although VandenAkker et al. (2016) did not find differences in peptide building blocks. As acid hydrolysis is rate-limiting at pH 2.0, and the initial aggregation rate was increased by using larger protein concentrations, it is hypothesized that the resulting worm-like aggregates are formed from intact BLG or longer peptides, in which N- and C-terminal peptides might be linked through native disulfide bonds.

In addition to the pH value and protein concentration, ions affect the BLG amyloid morphology. This is due to charge screening effects (i.e., lower electrostatic repulsion), but also to direct binding to the protein. Amyloid aggregation at acidic pH values and elevated temperatures can be accelerated by the addition of salt, which generally leads to a shift towards worm-like aggregation due to more random association (e.g., >50 mM NaCl at pH 2.0; Arnaudov, de Vries, Ippel, & van Mierlo, 2003). Similar to the worm-like aggregates at pH 3.5 or at high initial protein concentration, these aggregates are more flexible. Loveday et al. (2010) found that in the presence of ≥60 mM $CaCl_2$ or ≥33 mM NaCl, L_c is a few hundred nanometers and L_p is 38–84 nm, while in the absence of salt, L_c is 0.5–1 μm and the L_p of 1.8–4.3 μm. They reported that both monovalent (NaCl) and divalent ($CaCl_2$) ions accelerate the growth of fibrils to a comparable extend, leading to similar morphologies, while only divalent ions accelerate the nucleation, presumably through bridging between peptides. Similarly, Zappone, De Santo, Labate, Rizzuti, and Guzzi (2013) observed a longer lag phase for BLG fibril formation in the presence of copper (Cu^{2+}) without affecting the fibril growth much. Copper destabilizes BLG, which leads to earlier unfolding upon heating (i.e., decreased denaturation temperature), and may initiate sulfhydryl oxidation and disulphide exchange reactions. An equimolar addition of copper to BLG resulted in fibrils with a larger diameter due to increased interfilamentous association. Further addition of cupper (1:10 mol/mol) resulted in the formation of additional fibrils with a smaller diameter (~1 nm), probably due to the stabilization and elongation of smaller nuclei that otherwise would fall apart (Zappone et al., 2013). Similarly, zinc also accelerates fibril formation through destabilization of BLG, which in contrast to copper leads to unfolding prior to heating, through further opening of the disulphide bond conformation (~50% for Zn-BLG and ~25% for Cu-BLG). In addition, zinc is more effective in redistribution of charges, which led to bigger (up to 65 nm instead of 50 nm) and slightly branched fibrils during heat-induced aggregation (Navarra et al., 2014).

2.2. Post-aggregation

Once mature amyloids are formed, their morphology can be modified by changing the environmental or processing conditions, for example, through continued acid hydrolysis during prolonged incubation. Even though it is assumed that worm-like aggregates consist mainly of intact BLG at pH > 3.0, Keppler, Heyn, Meissner, Schrader, and Schwarz (2019) showed that BLG is partly hydrolyzed at pH 3.5 at 90 °C (0–24 h). This hydrolysis proceeded at prolonged incubation times, while the relative number of intermolecular β-sheets had already stabilized (1–2 days). This was postulated to be due to 'shaving' of aggregates. In essence, this is the removal of peptide sequences that are not involved in the intermolecular aggregation, but which were linked to peptide sequences that were. One could expect a morphological change towards the semi-flexible fibrils since the building blocks change towards peptides, but this was not the case, which indicates that the two types of aggregates differ in their core segments.

Extended heating times may cause individual BLG fibril filaments to associate into twisted or helical filament bundles (Fig. 3; Adamcik & Mezzenga, 2018). For example, two or more single filaments (~2.6 nm diameter) associated into thicker fibrils (~4.0 nm diameter) after 96 h of incubation at 80 °C and pH 2.0 (VandenAkker et al., 2011). A higher tendency for this association was observed when increasing the incubation pH from 2.0 to 4.0 (Jung, Gunes, & Mezzenga, 2010). At pH 2.0 and 90 °C, maximally five filaments interacted for incubation times up to 5 h, with up to 16 strands after 30 h of incubation (Lara, Adamcik, Jordens, & Mezzenga, 2011). Interestingly, the heterogeneity of the number of filaments included in the fibrils was higher when produced with conventional heating, as compared to microwave-assisted heating. This was attributed to the need for heat transfer in conventional heating, as compared to instant heating by microwave-induced rotation of water molecules (Lee et al., 2015).

Association of the BLG filaments into bundles (Fig. 3) occurs through hydrophobic short-range attractions, while long-range electrostatic repulsions lead to a twist in the fibril that has a periodic pitch (i.e., twist frequency). Therefore, the addition of NaCl to mature fibrils leads to a longer pitch (Bolisetty, Adamcik, & Mezzenga, 2011). A slightly longer pitch was also observed at higher temperatures (100–120 °C) (Loveday, Wang, Rao, Anema, & Singh, 2012). Similarly, Lee et al. (2015) found amyloid aggregates with a longer pitch and a lower surface charge density when heating with a microwave at 100 °C, as compared to heating to 70–80 °C. The authors hypothesized that the stacking mechanism at higher temperature resulted in more stable aggregates.

Amyloid aggregates prepared at acidic pH are often exposed to and stored at higher pH values for application in food, which results in a morphological shift. A pH adjustment to pH 4–6 induced semi-flexible BLG fibrils to aggregate into unordered aggregates, due to the lower interfibrillar electrostatic repulsion around their isoelectric point of 5.2 (Jones et al., 2011; Karbasi et al., 2021; Peng, Yang, Li, Tang, & Li, 2017). In addition, the fibrils became more flexible and shorter due to the progressive reduction in intrafibrillar electrostatic repulsion (Jones et al., 2011; Peng et al., 2017). In contrast, addition of NaCl to mature semi-flexible BLG fibrils did not change the morphology of the individual filaments but did increase the interfilamentous association (Adamcik & Mezzenga, 2011). Peng et al. (2017) reported that a further pH adjustment to 7.0 allowed for an increased electrostatic repulsion that opened the aggregates, resulting in alignment of the fibrils (Fig. 3). In addition, exposed sulfhydryl groups might form intermolecular disulphide bonds, which become more reactive at higher pH. At the acidic pH usually applied for amyloid formation, sulfhydryl groups are less reactive due to protonation, although it remains unclear whether that completely avoids intermolecular disulphide bond formation.

2.3. Amyloid aggregation of other food proteins

Several food proteins possess 'core regions', i.e., specific amino acid regions that are prone to amyloid aggregation under sufficiently long aggregation times (Jansens et al., 2019). Slow aggregation is induced under specific conditions, depending on the protein sequence, folding and stability. Goldschmidt, Teng, Riek, and Eisenberg (2010) showed that at least 98.7% of all proteins contain a core region that can form intermolecular β-sheets. It can therefore be assumed that amyloid aggregation is a generic protein property. In the following, a selection of proteins that show similar morphologies or interesting differences to BLG are described.

Similar to BLG, worm-like aggregates and semi-flexible fibrils can be

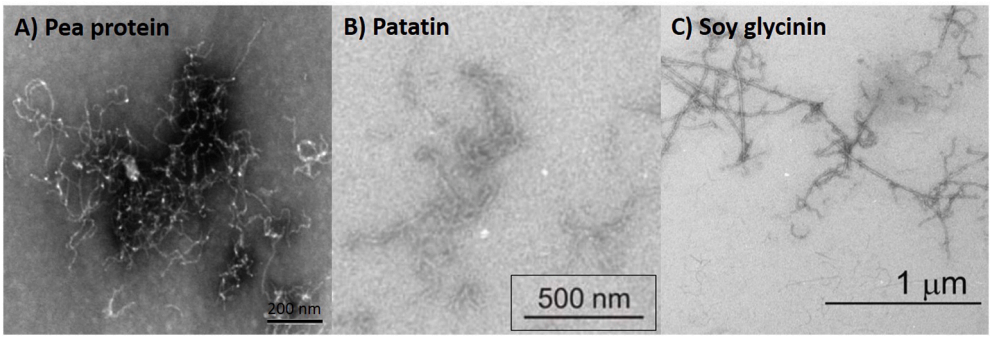

Fig. 3. Modification and assembly of amyloid (-like) aggregates into higher order networks.

formed from several animal proteins under similar conditions described in section 2.1. Usov, Adamcik, and Mezzenga (2013) reported simultaneous worm-like aggregate and semi-flexible fibril formation for BSA (6 wt% at 90 °C and pH 2). Short ($L_c \sim 0.5$ μm) and worm-like ($L_p = 0.15–16$ μm) aggregates were formed initially (≤40 h), with long ($L_c \sim 2.2$ μm) and semi-flexible ($L_p = 1.3–2.6$ μm) fibrils being additionally formed during prolonged heating times (up to 145 h). They proposed that worm-like BSA aggregates are converted into semi-flexible fibrils during prolonged heating, by converting the twisted filaments into nanotube-like structures. A similar aggregation behavior has been shown for ovalbumin by Lara et al. (2011). Flexible worm-like aggregates ($L_p = 63 \pm 7$ nm) were formed within the first few hours, followed by bendable ($L_p = 300 \pm 80$ nm), longer filaments formed after around 2 h. After approx. 6 h of incubation, filaments intertwined to form rigid ($L_p = 3000 \pm 700$ nm) fibrils. Longer incubation times resulted in shorter contour lengths and addition of salt resulted in a shift towards longer worm-like aggregates, while the other morphologies were almost non-existent. Gosal et al. (2005) proposed that different amyloid forming pathways compete, resulting in either the worm-like aggregate or semi-flexible fibril structures. For the human amyloid protein β2-microglobulin (β2m) they propose that fast kinetics in which no lag phase is observed result in worm-like morphology, while slow kinetics with a lag phase result in semi-flexible fibrils. Similar to BLG, β2m forms flexible, short ($L_p = 50$), and worm-like aggregates (at pH 3.5 in the presence of 200 mM NaCl). In addition, β2m forms rigid, long ($L_p = 1740$), and semi-flexible fibrils that consist of multiple filaments, at pH < 2.5 in the absence of NaCl. A shift towards semi-flexible fibrils can be induced by removing the nucleation barrier through changes in the solution conditions (e.g., decrease in pH), addition of seeds, or agitation.

In comparison to fibrils from animal proteins, a lower resemblance to semi-flexible BLG fibrils is observed for fibrils from plant storage proteins, such as pea protein, patatin, and soy protein, since they are often branched (Fig. 4). Heating pea protein at pH 2.0 and 85 °C resulted in short and worm-like aggregates that present a certain degree of

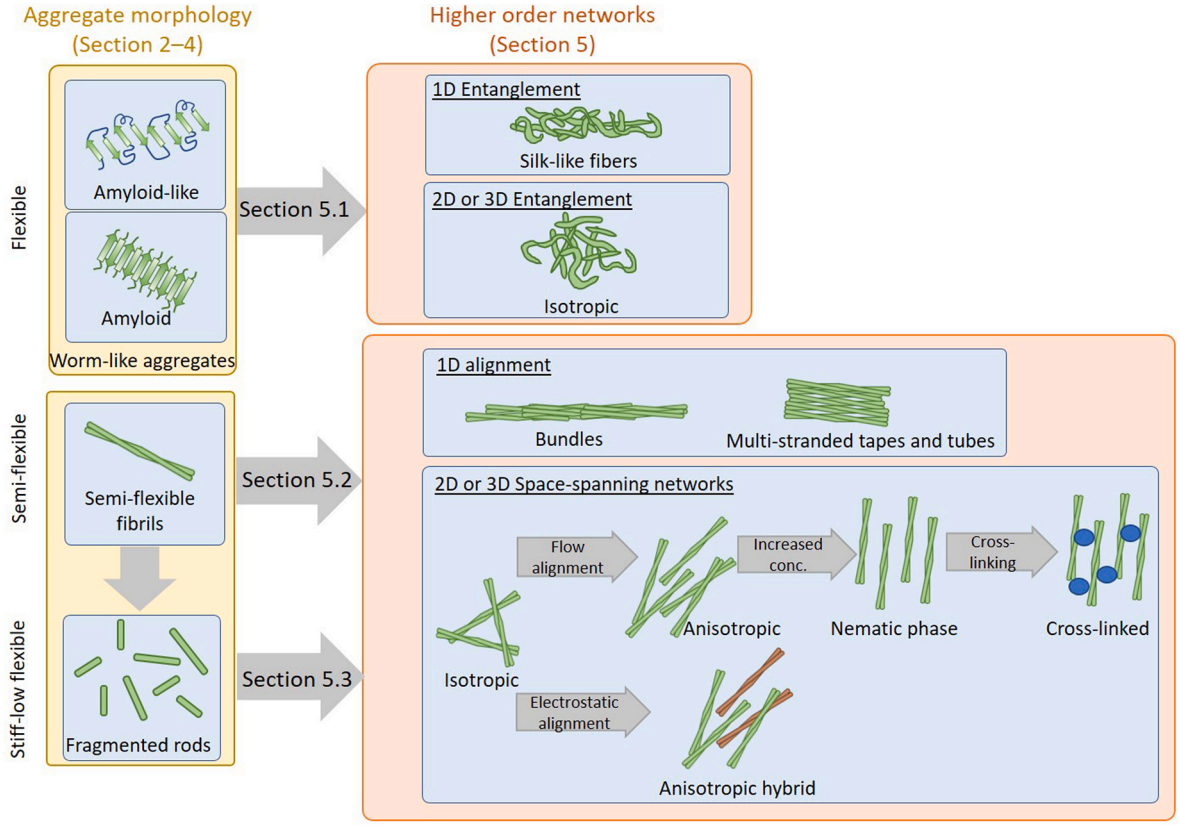

Fig. 4. Amyloid aggregates prepared from (A) 4 wt% pea protein (20 h at pH 2.0 and 85 °C, taken from Munialo et al. (2014), (B) patatin (prolonged heating at pH 2.0 and unknown temperature, taken from Akkermans (2008), and (C) 4 wt% soy glycinin (20 h at pH 2.0 and 85 °C, taken from Akkermans et al. (2007).

branching (Munialo, Martin, Van Der Linden, & De Jongh, 2014), in contrast to the unbranched semi-flexible fibrils formed from BLG under these conditions. Patatin also forms short (~0.5 μm) worm-like aggregates at pH 2.0. Likewise, soy glycinin forms branched amyloids (20 h, pH 2.0 and 85 °C). However, their flexibility is more comparable to BLG fibrils and they are longer ($L_c = 0.1–4$ μm ≈ Lp; Akkermans et al., 2007). Amyloids from soy protein isolate (80% soy glycinin, 20% β-conglycinin) are similar to the ones from soy glycinin but show a higher degree of branching (i.e., lower birefringence signal). It remains unclear what causes this branching, but plant proteins in general contain a relatively low amount of charged residues (Day, 2013), which might increase their tendency to assemble at multiple locations at the protein or peptide. Lastly, wheat gluten is also shown to form unbranched fibrils as well as non-amyloid aggregation upon heating at 78 °C for 22 h or boiling for 15 min. However, enzyme treatment was performed to remove non-fibrillated protein, which might have an impact on the fibril morphology (Monge-Morera et al., 2021).

3. Further physical processing conditions

Processing and storage of fibrils in specific environments can lead to morphological changes. Below we will discuss studies that demonstrate the considerable influence of the mechanical energy input and change of the interfacial energy on the amyloid aggregates. These aspects destabilize the initial non-aggregated protein structure, accelerate the denaturation, and influence the morphology of the already aggregated structures.

3.1. Mechanical stress and shear field

Mechanical stress (e.g., shear forces, cavitation or high- or dynamic pressure application) is both an aggregation and post-aggregation factor. Shear stress can irreversibly or reversibly change the protein conformation, and results in an increased aggregation tendency without affecting the resulting morphology (Heyn et al., 2020). Fibrillization is generally regarded to follow a nucleation-dependent polymerization mechanism, which consist of nucleation and elongation (Chatani et al., 2009). The nucleation rate is affected by the corresponding shear flow, as protein-protein collisions are either induced (turbulent flow) or prevented (laminar flow). For BLG, conformational changes were described at shear rates up to 1000 s^{-1} in combination with acid pH and high temperature (Rahaman, Vasiljevic, & Ramchandran, 2015). Cavitation and simultaneously generated air-water interfaces can stimulate a globular protein to unfold and to aggregate (Wang, Nema, & Teagarden, 2010). They also locally affect nucleation by inducing and preventing spatial assembly of proteins, thereby having an impact on nucleation and fibril growth.

The mechanical energy input and corresponding flow plays an important role in aggregate nucleation and growth. In general, shearing of BLG solutions by shear rheometers, magnetic stirrers, or four-roller apparatus, can shorten the lag phase, accelerate subsequent growth and affect fibril yield and length (Akkermans et al., 2006; Akkermans et al., 2008; Bolder, Sagis, Venema, & Van Der Linden, 2007; Dunstan, Hamilton-Brown, Asimakis, Ducker, & Bertolini, 2009). Similarly, shear pulses have been shown to cause accelerated nucleation (Akkermans et al., 2006). Akkermans et al. (2008) explained the increased kinetics by the enhanced transport of potential building blocks to the active nucleus end, due to the implemented shear field. Even though the impact of shear on the BLG fibril morphology has not been reported extensively in literature, effects were described for other proteins. For the fibrillization of the protein glucagon, a minimum mechanical stress (e.g., by agitation speed) can lead to two different fibrillar morphologies (MacChi et al., 2011). Fibrils created at low stress were mostly straight, modestly twisted and tended to associate laterally. Fibrils created at high stress were very straight, showed a pronounced twist and did not associate laterally. The importance of mechanical stress for the occurrence of polymorphism was also noted for fibrils from Aβ-peptide (Petkova et al., 2005) and prion proteins (Makarava & Baskakov, 2008). Greving, Cai, Vollrath, and Schniepp (2012) demonstrated that shear can result in the formation of self-assembled nanofibrils from native silk protein during spin coating, prior to drying. The fibril diameter decreased with the protein concentration (0.1% compared to 10%, w/w).

Mechanical stress mainly influences the fibrillization mechanism through fragmentation and secondary nucleation. Fragmentation of protofibril structures in the shear field, e.g., during stirring (Bolder, Sagis, Venema, & Van Der Linden, 2007; Dunstan et al., 2009; Heyn et al., 2020) or ultrasound application (Sneideris, Milto, & Smirnovas, 2015), results in release of new active ends. These so-called 'seeds' are available as nuclei that can subsequently grow into fibrils (Dunstan et al., 2009). Nicoud, Lazzari, Balderas Barragán, and Morbidelli (2015) reported that upon increased agitation (50–250 rpm), fragmentation reactions are accelerated about eight times more as compared to fibril growth, which therefore leads to a lower average length of fibrils. The breakage pattern remained the same, while thermal breakage shifts from an erosion (i.e., at fibril ends) to random breakage at lower temperatures, for both BLG and insulin.

The influence of mechanical stress on fibrils as a post-aggregation factor is particularly relevant in the context of the manufacturing processes of (food) products. In such processes, different mechanical stresses act on the fibrils. For example, the application of rotor-stator dispersion and high-pressure homogenization, as used to produce stable oil-in-water emulsions, strongly affects the fibril size (Serfert et al., 2014; Uttinger et al., 2020). Cavitation by ultrasound (Mantovani, de Figueiredo Furtado, Netto, & Cunha, 2018) or dynamic high-pressure treatment (Serfert et al., 2014) leads to even stronger fragmentation of mature fibrils into fibers of 80 and 90 nm. Thus, such processes can also be intentionally used for post-processing of fibrils, as the resulting fragments have a homogenous length and are less flexible than intact fibrils.

The decrease in mean fibril length depends almost directly on the applied mechanical energy intake. Heyn et al. (2021) showed that semi-flexible fibrils (pH 2.0) and worm-like aggregates (pH 3.5) from BLG were only partly dissociated upon energy intakes up to 76 J mL^{-1} min^{-1}, as applied by ultra-sonication. Fragmentation of worm-like aggregates from BLG was less pronounced than for semi-flexible fibrils, when the mechanical stress was applied by rotor-stator disperser, probably due to the higher flexibility, and larger homogeneity of the stress over the fluid. Static high-pressure of lysozyme fibrils above 450 bar can lead to fibril or filament dissociation, which may be due to hydration of pressure-sensitive water-excluded cavities and hydrophobic pockets in the fibril structure (Radovan, Smirnovas, & Winter 2008).

3.2. Solid and liquid surfaces/interfaces

Interfaces can induce unfolding, adsorption and alignment of proteins. Therefore, a liquid or solid interface can induce aggregation of BLG. Even though it remains unclear whether it can induce amyloid aggregation of BLG, such effects were found for other proteins like insulin (Lee, Um, Park, & Park, 2008) and Aβ-peptide (Moores, Drolle, Attwood, Simons, & Leonenko, 2011). In the latter example, exposure to a hydrophobic solid surface (beads) promoted spherical amorphous aggregates, while charged surfaces induced anisotropic fibril formation. Similar effects were observed for immunoglobulin by Zhu, Souillac, Ionescu-Zanetti, Carter, and Fink (2002): the negatively charged surface of mica promoted fibril formation. Interestingly, this was not the case with mica that was positively charged or modified to have a non-polar surface. It was stated that the growth mechanism on solid surfaces accelerates fibril formation, as compared to aggregation in solution. Fibrillization of immunoglobulin at the surface can occur through bidirectional linear assembly of building blocks, or through linear growth from amorphous cores. Lastly, the deposition of a water droplet

on a heated super hydrophobic surface can induce fibril formation into different morphologies, as shown for disease related proteins (Tau and PHF6 peptide) and lysozyme. At temperature gradient of 20 °C, short fibrils were formed, while higher temperature gradients resulted in longer fibrils. The growth process and resulting fibril morphology varied, depending on the temperature gradient, the movement time within the flows until the droplet evaporates, and the de-pinning process (Zhang et al., 2020).

Surfaces and interfaces can also function as a post-processing factor to modify the fibril morphology. Heat-induced semi-flexible BLG fibrils tend to curve into rings and loops when exposed to liquid interfaces (air-water and oil-water). The stress caused by bending, high surface tension or exposure to air can result in fracturing of the fibrils (similar to mechanical fragmentation, section 3.1.). The resulting shorter fibrils can also bend and form rings at a liquid interface. In addition, they can assemble in or on existing rings, either in a parallel or perpendicular fashion (Jordens et al., 2014). It is unclear whether these rings remain stable during foaming or drying.

As discussed in section 3.1, seeds can accelerate fibril formation. This effect could be regarded as a surface effect, because "seeds" can act as a solid surface to promote self-association. Seeds can aggregate with surrounding proteins, which favors conformational changes in the proteins and may lead to subsequent exposure of hydrophobic groups. This accelerates the ordered aggregation. In addition, the seeds act as a template for the conformational changes induced and thereby can be used to tune the morphology (Vetri & Foderà, 2015).

The effects of surfaces on the self-association are also evident in the drying of fibrils. Using the Langmuir-Schaefer deposition technique, Smith, Fernandez-Rodriguez, Isa, and Mezzenga (2019) describe that soft/flexible fibrils tend to de-wet at the water-air meniscus due to capillary forces. These capillary forces occur at the receding meniscus during drying. This can cause aggregation of the fibrils into higher order structures (section 5). The surface tension influences this change in the receding meniscus. Thus, with regard to preventing morphology changes upon the transfer of fibrils from a liquid-liquid interface to a solid substrate, low viscous and volatile excipients that lower the surface tension but do not affect fibril morphology, such as hexane, are needed (Smith et al., 2019).

4. Further chemical environmental conditions

As previously described, the fibril properties can be modified by adaptation of the physical processing conditions. Likewise, the physicochemical conditions can accelerate or inhibit amyloid aggregation, and modify the properties after aggregation.

4.1. Denaturants and surfactants

Protein unfolding is one of the critical steps observed in amyloid aggregation, which is often achieved through elevation in temperature (section 2.1). Alternatively, denaturants (e.g., guanidine chloride or urea) can be used to reduce intra- and intermolecular interactions, through direct interaction with the protein or changing the solvent quality (Hamada & Dobson, 2009; Stumpe & Grubmüller, 2007; L.; Zhang & Schmit, 2017). For example, urea can displace water at the interface of proteins, weaken hydrophobic interactions, and subsequently induce unfolding indirectly. Besides, it can solvate the peptide backbone, exposing polar and aromatic residues, leading to further unfolding (Stumpe & Grubmüller, 2007). Unfolding of the protein results in exposure of aggregation-prone structures that stimulates the tendency for aggregation. However, intermolecular interactions are decreased simultaneously, which results in destabilization of the aggregates when formed. Whether these effects will result in an accelerated or decelerated fibrillization, depends on the denaturant, its concentration, and the type and stability of the protein. In the presence of 3–5 M urea, BLG can form unbranched semi-flexible fibrils (8–10 nm diameter) at neutral pH after incubation for 1 month (37 °C). Urea concentrations below 3 M and above 5 M prevent the formation of amyloid aggregates. At concentrations of <3 M, the dimer is stabilized, and unfolding is limited. Fibrils prepared with 3 M urea contained some thicker fibrils (~15 nm) as compared to fibrils formed with 4 and 5 M urea (~8–10 nm) (Hamada & Dobson, 2009).

The surfactant sodium dodecyl sulphate (SDS) is commonly used to destabilize the native conformation of proteins by neutralizing charges and inducing hydrophobic interactions. Khan et al. (2012) used SDS (100-fold molar excess) to induce aggregation of several proteins at a pH that was 2 units below or above the pI. Above the pI, SDS and the proteins were both negatively charged, preventing interaction of SDS with the proteins, thereby avoiding aggregation. Below the pI, amyloid aggregates were formed with different morphologies depending on the protein. They ranged from worm-like amyloids to semi-flexible fibrils, and varied in branching, size, and degree of interfibrillar aggregation. Jung et al. (2008) prepared heat-induced semi-flexible fibrils (pH 2.0) and worm-like aggregates (pH 7.0) from BLG and observed the complexation with SDS upon a pH shift to 3.0. SDS neutralized the charge of the amyloid structures, resulting in precipitation. However, upon a further increase in SDS, a double layer was formed that resulted in redispersion of the aggregates (including at the isoelectric point, as discussed in section 2.2.). Other surfactants ($>10^{-3}$ M), such as fatty acids or soy lecithin, can also hydrophobically interact with peptides or proteins. Mantovani, Fattori, Michelon, and Cunha (2016) found a decreased yield for heat-induced fibrillization of WPI in the presence of soy lecithin, without affecting the fibrillization rate or the resulting morphology. Above the critical micelle concentration (CMC) of lecithin, fibril aggregation was stimulated, possibly through an excluded volume effect.

4.2. Solvents

Apart from denaturants and surfactants, solvents such as ethanol can also induce unfolding (indirectly) through destabilization of the protein, and thereby promote aggregation. Solvent-induced fibrillization has a clear impact on the morphology (Kayser, Arnold, Steffen-Heins, Schwarz, & Keppler, 2020; Liu, Li, Qin, & Zhong, 2021; Yoshida et al., 2012). In contrast, substances that stabilize the tertiary structure, such as glycerol (plasticizer), will likely hinder the aggregation without altering the morphology (Dave, Loveday, Anema, Jameson, & Singh, 2014b).

Many solvents partly denature BLG, which is then followed by a transition into a predominant β-sheet conformation via an initial stage of α-helical conformation (Kayser et al., 2020; Yoshida et al., 2012). At high protein concentrations, this mechanism can be followed by amyloid-like aggregation (Yoshida et al., 2012). Solvents that were already found to affect the amyloid aggregation of BLG at various conditions (e.g., temperature, pH value) are 2,2,2-trifluoroethanol, 3,3,3′, 3′,3′-hexalfluoro-2-propanol, methanol, ethanol and propane-2-ol (Gosal, Clark, Pudney, & Ross-Murphy, 2002).

Worm-like aggregates, consisting of mainly intact proteins instead of closely assembled β-sheet peptides, can be obtained in the presence of hydro-ethanolic solutions, for example, at low temperatures up to 30–50 °C (Kayser et al., 2020). Due to the more non-polar environment compared to purely aqueous solutions, hydrophobic forces become less relevant, while hydrogen bond strength increases. The polarity is determined by the solvent type (e.g., dimethyl sulfoxide [DMSO], ethanol, or methanol) and its volume, affecting the hydrophobicity and binding mode. In addition, temperature elevations affect the polarity (i.e., through the dielectric constant), but also the protein-solvent interactions (i.e., binding) and the protein mobility. Consequently, a lower solvent concentration is required to induce amyloid aggregation at increased temperatures. The effect of solvents on the aggregate morphology is time dependent. Kayser et al. (2020) observed spherical aggregates (no amyloids) immediately after the addition of ethanol,

DMSO or methanol (30%, v/v, 30 °C). After 5 h of incubation, both spherical and worm-like aggregates were present. At higher temperature, both worm-like aggregates and semi-flexible fibrils were formed in the presence of ethanol (10–50%, v/v, 85 °C; Liu et al., 2021). Interestingly, solvent-induced aggregates vary in their morphology, which could potentially be used to shape these aggregates. For example, DMSO-induced aggregates were found to be slightly longer (100–150 nm) than ethanol-induced aggregates (20–60 nm) (Kayser et al., 2020).

Exposure to solvents can be used as a post-aggregation factor. Jordens et al. (2011) mixed heat-induced semi-flexible BLG fibrils with ethanolic solutions (10–50%, v/v) and incubated (37 °C) them for several weeks. Initially the semi-flexible fibrils (~2.4 μm in water) changed their morphology into worm-like aggregates (29.43 nm in the presence of 50% ethanol for 1 week). These consisted of peptides as building blocks with an increased concentration of random coil and turn elements, and lost their multistrand character (2.5–2 nm, instead of 4–10 nm). Upon longer incubation, the contour length of the worm-like aggregates grew (up to 550 nm in 8 weeks) at the expense of the semi-flexible fibrils. A critical concentration of 30% was necessary for the described transformation.

4.3. Oxidants and reductants

Different chemical modifications of BLG can be induced through oxidation reactions. Protein oxidation is a generic term for the covalent modification of proteins through chemical reactions with reactive oxygen, nitrogen or sulphur species (Hellwig, 2019). Depending on the nature of the oxidant and the oxidation mechanism, amino acids can be chemically modified, mainly through the formation of carbonyls, hydroperoxides and sulphur oxides. These modifications can lead to changes in charge and hydrophobicity, crosslinking of sulphide or tyrosine, cleavage of disulphides and/or backbone cleavage (Davies, 2016). Consequently, destabilization and (partial) unfolding can lead to aggregation (Davies, 2005). Thus, protein oxidation is an aggregation factor. From a technological point of view these effects can modulate the functional properties of the proteins (Hellwig, 2019).

A different folding of proteins through oxidative stress and subsequent oxidative modifications can favor and promote amyloid aggregation *in vivo,* which is related to neurodegenerative disorders (Cheignon et al., 2018; Gregersen, Bolund, & Bross, 2003). Effects of oxidation on the protein structure may induce similar effects compared to the effects occurring under extreme conditions (e.g., urea, high temperature and low pH; see section 2) resulting in hydrolysis and unfolding. This demonstrates the potential of oxidation reactions for the targeted production of amyloid aggregation. Oxidation reactions during the aggregation process itself (90 °C, pH 2 or pH 3.5) can change the building blocks of amyloid aggregates of BLG and thus affect the resulting morphology and functionality of the aggregates (Keppler et al., 2019). Recently, Maity et al. (2021) reported that selective methionine oxidation in BLG leads to a more flexible and unfolded state, which is more prone to fibrillization. Heat-induced aggregation at physiological pH lead to worm-like aggregates (40–55 nm diameter) for native BLG, while more fibrillar aggregates were obtained for oxidized BLG (20–35 nm diameter).

Reduction reactions also affect amyloid aggregation. For BLG, Hamada and Dobson (2009) only found monomeric species in urea-induced BLG fibrils, indicating the absence of intermolecular disulphide bonds. For temperature-induced fibrillization, it remains unclear whether intermolecular disulphide bonds are formed. However, intramolecular disulphide bonds play a major role in amyloid aggregation. Under similar conditions, Hamada et al. (2009) showed that certain BLG peptide sequences (βG, βH, and βI strands) are hindered to form amyloid structures, due to a conformational restraint induced by disulphide bonds. Reduction and carboxymethylation of BLG (RCM-BLG) therefore resulted in more fibril formation. Two types of fibrils were formed for RCM-BLG, i.e., semi-flexible fibrils (~14.7 nm diameter) and worm-like aggregates (~10.2 nm diameter), while intact BLG showed a uniform semi-flexible fibril morphology (~16.9 nm diameter). The difference in morphology was explained by the exposure of further regions in RCM-BLG that could initiate nucleation. Seeding experiments with peptides from the different region of BLG confirm that this results in a shift in the morphology.

4.4. Ligands: phenolic compounds and sugars

BLG can be modified by association or reaction with other compounds (mainly by phenolic compounds and sugars), which will change the amyloid building blocks and subsequently influence the amyloid formation kinetics and resulting morphology. In addition, phenolic compounds can inhibit protein oxidation (section 4.3) through their antioxidative property, and is also shown to inhibit pathogenic Aβ aggregation in vitro (Hamaguchi, Ono, Murase, & Yamada, 2009).

Interaction of proteins with phenolic compounds indeed inhibits amyloid aggregation. The flavanoid rutin binds in the hydrophobic core of BLG, decreasing the solvent accessibility and thereby decelerating amyloid aggregation, without completely preventing it (Al-Shabib et al., 2019). Curcumin and its derivatives can also bind with BLG monomers, destabilizing them or blocking potential aggregation sites (Maity et al., 2018). Resveratrol hydrophobically binds with BLG, inducing a slight opening of the hydrophobic cavity (Ghorbani Gorji et al., 2015). This changes the conformation, increases the hydrophobicity, and thereby leads to amorphous BLG aggregates instead of amyloid aggregation (pH 2.0 and 70 °C; Ma, Zhang, Liu, Xie, & Wang, 2018). The effect of the fibrillization of ovotransferrin by phenolic compounds depends on whether it is covalently bound or not. Wei and Huang (2020) reported that total fibrillization was inhibited for ovotransferrin in the presence of (covalently and non-covalently bound) epigallocatechin-3-gallate (EGCG). Interestingly, the fibril thickness was unaffected when EGCG was covalently bound, while the fibril length was further reduced (from 327 to 78–102 nm), when compared to non-covalently bound EGCG (from 327 to 322–312 nm). Non-covalently bound EGCG led to fibrils with larger diameter. The same was observed for gallic acid (Wei & Huang, 2019). Similar to EGCG, covalently bound gallic acid reduced the L_c (327–92–127 nm), while non-covalently bound gallic acid did not affect the L_c. The fibril diameter increased with covalently bound gallic acid (6-filament instead of 2- and 4-filament from native protein), as compared to non-covalently bound gallic acid (3-filament). The zeta-potential, surface hydrophobicity, rheological properties, antioxidant activity and digestion of the fibrils was affected differently as well. The addition of phenolic compounds can also act as a post-aggregation factor: Maity et al. (2018) reported the disruption of amyloid-like aggregates (prepared at 75 °C and pH 7.4) into smaller oligomers (<120–130 nm compared to ~ 140–150 nm) upon incubation with curcumin and its derivatives for 24 h.

BLG functional side groups (i.e., sulfhydryl, amino, carboxylic acid, and hydroxyl groups) can also be covalently modified with other compounds. For example, citraconylation of amino groups in lysine residues neutralizes the electrostatic repulsion between BLG monomers, which reduces the BLG stability and enhances fibrillization. TEM imaging shows that the morphology remains similar (Figure6 in Ghadami, Khodarahmi, Ghobadi, Ghasemi, & Pirmoradi, 2011). Similarly, glycation (glucosylation and lactosylation) can lead to charge neutralization and accelerates protein unfolding. However, the stimulating effect of the decreased electrostatic repulsion on fibrillization upon glycation is often outweighed by the steric hindrance and introduction of hydrophilic side groups, which results in the disruption of the amyloid structures. Therefore, the fibrillization kinetics were slowed down (Zhao et al., 2020), while the morphology remained unchanged (Dave, Loveday, Anema, Jameson, & Singh, 2014a). In contrast, *in vivo* glycation of proteins has been often reported to stimulate fibrillization, most likely through the formation of advanced glycation end-products (AGEs) that are prone to cross-linking. Da Silva Pinto et al. (2012) and Zhao et al.

(2020) reported disulphide bond formation within and between fibrils from glycated BLG. This is accompanied by a morphological shift from fractal to worm-like amyloid aggregates. For lactosylation of WPI, Liu and Zhong (2013) reported that the fibrillization rate remains unaffected, while the fibril yield is reduced. Interestingly, glycated WPI fibril solutions remained transparent upon changes in pH (3.0–7.0) and salt addition (0–150 mM NaCl), and the fibrils were heat stable. Sugars can be added to fibrils post-aggregation to enhance fibril functionality: Karbasi et al. (2021) showed that modification of BLG fibrils with maltodextrin leads to an increased colloidal stability at pH 4.0 by inducing steric hindrance, while maintaining the fibril morphology.

5. Multidimensional amyloid networks formed as a function of the morphological diversity

The usefulness of fibrils in different applications is determined by their spatial arrangement in one-dimensional alignment (1D) or two- or three-dimensional networks (2 and 3D). Such networks can be fibers that are entangled into higher order bundles (1D), onto surface coatings and into films (2D) or gels (3D networks) (Schleeger et al., 2013; Wei et al., 2017). The mechanical stability of these systems depends on the ability of the fibrils to align or interlock with each other. Which of these properties dominates depends primarily on the fibril morphology (i.e, their flexibility and length). Further tunable properties such as their surface hydrophobicity, the intermolecular interactions, and their surface charge affect the rheological behavior of the fibrillar matrix (Schleeger et al., 2013). Thus, tuning the properties of the fibrils allows for a range of textural options (Fig. 3).

5.1. Networks made of flexible worm-like aggregates ($L_p < L_c$)

Aggregates have a highly flexible nature when their persistence length (L_p) is much lower than their contour length (L_c). Most worm-like BLG aggregates belong to that category (usually $L_p \sim$ 10–40 nm) (Table 1). In 1D orientation, purified short and flexible aggregates prepared at high protein concentration >6 wt% ($L_p \sim$ 41 nm, $L_c =$ 100–1000 nm; section 2.1) show poor alignment with flow, but superior entanglement in a microfluidics setup for flow induced hydrogel fiber production. These entangled fibers have higher mechanical strength than those observed for aligned semi-flexible fibrils. Indeed, similarities in the association mechanisms between recombinant spider silk proteins and worm-like amyloid aggregates are suggested (Kamada et al., 2017).

In 2D applications, amyloid (-like) structures arrange in planar orientation and can result in Pickering type stabilization. Besides, highly flexible ethanol-induced worm-like BLG aggregates (section 4.2) were found to have a high surface adsorption rate and packing density on the oil droplet surface, which increased the thermal stability of emulsions (Liu et al., 2021). Interfaces stabilized by worm-like aggregates have a higher surface shear modulus than those stabilized by semi-flexible fibrils, although the complex shear modulus of worm-like aggregates was significantly lower (Humblet-Hua, Van Der Linden, & Sagis, 2013, section 5.2.1).

In 3D orientation, highly flexible, curly pea protein amyloids yielded a lower gel strength than semi-flexible WPI fibrils, which was attributed to the higher flexibility of the pea protein amyloid aggregates and thus their lower degree of alignment (Munialo et al., 2014). Short and flexible salt-induced worm-like WPI aggregates (section 2.1) were likewise reported to have a lower capacity to enhance the bulk viscosity than semi-flexible fibrils at pH 2.0, because of their short and irregular morphology. Fibrils made in the presence of $MgCl_2$ and $BaCl_2$ could create networks at somewhat lower concentrations than those prepared in the presence of LiCl and KCl. Although all aggregates were worm-like and flexible, it was hypothesized that $MgCl_2$ and $BaCl_2$ fibrils could be slightly longer and thus show better alignment capacity. Difference in the surface properties are also likely (Loveday, Su, Rao, Anema, & Singh, 2012).

5.2. Networks made of straight amyloid aggregates ($L_P \approx L_C$)

5.2.1. Semi-flexible fibrils

For long, straight and semi-flexible fibrils L_p usually equals L_c or is close to it (Table 1). During 1D orientation (i.e., fibril bundles), flow alignment of semi-flexible fibrils was observed by Kamada et al. (2017). Semi-flexible BLG fibrils align to fibers of high mechanical stability during electrospinning in the presence of poly (ethylene oxide). The elastic modulus of these fibers was superior to those made from silk, collagen or gelatin. The fibrils were, however, already mechanically fragmented during mechanical mixing of the solution (L_c of approx. 1 μm), and the electrospinning process further reduced the size to ~97 nm (Chen, Narayanan, et al., 2020). Thus, the flexibility of the fibrils likely decreased during processing due to the size reduction.

Fibril bundles with increasing rupture stability and length can be prepared through association with other fibrous macromolecules, such as pectin. Because of weak interactions, the fibrils can slide within the hybrid-bundle into a more stable configuration. A wide range of structures and functionalities could be possible by varying the ratio of protein fibrils and carbohydrate fibrils (Loveday & Gunning, 2018). Likewise, the self-association of hen egg-white lysozyme and insulin in the presence of carbohydrate fibrils from gum arabic or pectin can already result in higher order fibrillar aggregates (Ow, Bekard, & Dunstan, 2018). Similarly, BLG can create ordered fibril structures that assemble into tapes (of 180 nm width) in the presence of pectin with a high degree of methyl esterification. These tapes are stabilized through electrostatic interactions (Hettiarachchi et al., 2016). Thus, hybrid materials are a promising route towards optimization of the functionality of semi-flexible fibrils.

Likewise, in 2D networks BLG fibrils align longitudinally in the film plane during the casting process, while they stack with nematic order in the presence of plasticizers (Knowles et al., 2010). Characterization of the mechanical properties of the films reveal, among other things, a Young's modulus that is similar to the rigid proteinaceous materials collagen and keratin. Semi-flexible straight fibrils align at an interface or surface which increases the complex shear modulus by an order of magnitude compared to short rigid fibrils (Humblet-Hua et al., 2013). In foams, fibrils generally anchor to the air-water interface. The comparatively lower foam stability of semi-flexible fibrils (pH 2; versus amorphous aggregates at pH 5) is explained by uneven attachment without forming a densely packed layer against coalescence (Peng et al., 2017), destabilizing the liquid film between bubbles. Oboroceanu, Wang, Magner, and Auty (2014) reported that polydisperse fibril systems that still incorporate unconverted material are most effective in stabilizing liquid interfaces. For the presence of longer fibrils, it is important to induce steric hindrance (Peng et al., 2017). Unconverted material is required to increase the viscosity of the liquid film. A similar synergy between fibrils and unconverted material is found for surface coatings of microcapsules and emulsions (Serfert et al., 2014).

In 3D networks, an increase in the concentration of semi-flexible fibrils induces a phase transition from an isotropic to a nematic phase above 0.4 wt% fibril, which is quantified by a 2D order parameter (Bolisetty et al., 2011). The addition of EGCG to semi-flexible fibrils that are already stacked in a nematic phase results in self-assembled hybrid supramolecular hydrogels through the well-known cross-linking capacity of the phenolic compounds via hydrogen bonds and hydrophobic interactions (Hu et al., 2018, Fig. 3). Associative interactions between semi-flexible whey protein fibrils and starch contributes to a synergistic increase in gel elasticity at low pH, but not at neutral pH conditions at which starch and protein are poorly compatible and may phase separate (Chen, Fang, Federici, Campanella, & Jones, 2020). Another example for hybrid materials is the composite gel created by BLG fibrils in combination with bacterial cellulose microfibrils (Peng et al., 2019).

5.2.2. Branched fibrils

Although branched fibrils are usually not observed with BLG (except

Table 1
Overview of aggregation conditions that lead to amorphous, worm-like, semi-flexible morphologies, or a combination, and the corresponding section where it is further discussed. The fibril morphology is described in terms of its persistence and contour length (L_p and L_c), and diameter (d). For the aggregation conditions, the aggregation temperature (T) and aggregation factors are listed. The colored rows represent the common aggregate structure of the respective category.

	Morphology			Aggregation conditions			Section	Reference
Main type	Described morphology	Lc (nm)	d (nm)	pH	T (°C)	Aggregation factor		
Amorphous aggregates	Monodisperse, compact and spherical	n.a.	150	5.8	85–90		2.1	Jung et al. (2008)
	Smaller		10–20	2	30–50	Solvent (30% ethanol)	4.1	Kayser et al. (2020)
			20–50	7	98	Ligands (maillard products)	4.4	Zhao et al. (2020)
			n.d.	7.4	75	Ligands (isoaxole)		Maity et al. (2018)
						Ligands (pyrazole)		
	Larger		150–400	7	RT	Oxidation (Ascorbic acid & H_2O_2)	4.3	Alavi, Momen, Emam-Djomeh, Salami, and Moosavi-Movahedi (2018)
			400–600	8–9				
			1000	8	37	Enzyme (endoproteinase AspN)	2.1	Akkermans et al. (2008)
Worm-like aggregate	Thin, short, worm-like and flexible (L_p ~10 nm)	50–200	1–3	3.5	90	n.a.	2.1	Heyn et al. (2019)
	Less flexible (L_p ~90 nm)	100–500	2.6	2	80	Concentration (7.5% BLG)	2.1	VandenAkker et al. (2011)
	Flexible (L_p ~ 41 nm)	100–1000	2.5 ± 0.5	2	90	Concentration (>6.0% BLG)	5.1	Kamada et al. (2017)
	More flexible	15–500	n.d.	2.0	30–50	Solvents	4.2	Kayser et al. (2020)
		100–500	2.7	2.0 and 7.0	RT			Gosal et al. (2004)
	Thicker	<100	6 ± 1	7	90	pH	2.1	Jung et al. (2008)
		100–300	thicker		98	Glycation	4.4	Zhao et al. (2020)
Aggregated and/or fragmented	Fragmented	100–110	n.d.	7.4	75	Ligands (curcumin diacetate)	4.4	Maity et al. (2018)
	Aggregated and fragmented	n.d.	n.d.	3.5	90	Prolonged heating (72 h)	4.3	Keppler et al. (2019)
	Aggregated	100	20	7		Glycation	4.4	Da Silva Pinto et al. (2012)
Semi-flexible fibrils	Thin, long, straight and semi-flexible (L_p = 3818 ± 164 nm)	200-5000	2.6	2	80	Concentration (3% BLG)	2.1	VandenAkker et al. (2011)
						Glycation	4.4	Dave et al. (2014)
								Liu and Zhong (2013)
						Surfactant (lecithin, < CMC)	4.1	Mantovani et al. (2016)
	L_p (~1960 nm)	100-1100	4.1 ± 1.1	2	90	concentration (<4% BLG)	5.1	Kamada et al. (2017)
	More curved and branched	n.d.	n.d.	2	90	Enzyme (Protease A, pepsin, protease M)	2.1	Gao et al. (2013)
	More flexible					Enzyme (Trypsin)		
	Thicker		thicker	4.6	80	Citraonylation	4.4	Ghadami et al. (2011)
			thicker	3.5	RT	Allura red (0.5–1 mM)	4.4	Al-Shabib et al. (2018)
Association of filaments		n.d.	~4	2	80	Prolonged heating (72 h)	2.2	VandenAkker et al. (2011)
	Homogeneous distribution	increase with wavelength			varied	Heating technique (conventional versus microwave heating)		G. Lee et al., 2015
	1-2 filaments	n.d.	1–5		80	Copper (1:10, mole BLG/cupper)	2.1	Zappone et al. (2013)
	2-3 filaments		4–6			Copper (Equimolar addition)		
	Longer pitch		n.d.	2	100	Temperature (microwave-assisted heating, control 70–80 °C)	2.2	G. Lee et al., 2015
Aggregated and/or fragmented straight fibrils	Aggregated	n.d.	n.d.	2	85	Rutin (30 μM)	4.4	Al-Shabib et al. (2019)
					80	Surfactant (lecithin, > CMC)	4.1	Mantovani et al. (2016)
	Fragmented and aggregated				90	Prolonged heating (72 h)	4.3	Keppler et al. (2019)
Mixture of morphologies	Both straight and worm-like structures	n.d.	1.02–1.47	7	37	Denaturant (5 M urea, 3 months)	4.3	Hamada and Dobson (2009)
			n.d.	2	80	Salt (≥60 mM CaCl2 or ≥ 33 mM NaCl)	2.1	Loveday et al. (2010)
		1000	50	8	80	Enzyme (AspN endoproteinase, pH shift to 2)	2.1	Akkermans et al. (2008)
	Shift towards more straight (self-seeded) or thinner fibrils (peptide seeded)	n.d.	1.46	7	37	Seeding (βA, βG and βH seeds) in 5M urea (3 months)	2.1	Hamada et al. (2009)
	straight and amorphous	120–130		7.4	75	Ligands (curcumin diacetate)	4.4	Maity et al. (2018)

Table 2
Overview of the effect of post-aggregation factors on specific morphologies, the morphological shift that occurs (diameter, d; persistence length, Lp; contour length, Lc) and the corresponding sections where it is discussed further. All aggregates were prepared at 80–90 °C and a BLG concentration of 1–4% (w/v).

Main type	Morphological shift	Aggregation pH	Post-aggregation factor	Section	Reference
Amorphous aggregates	SDS double layer prevents aggregation	5.8	Complexation with SDS (>1 mM), pH adjustment to isoelectric point	4.1	Jung et al., (2008)
Worm-like aggregates	Slightly fragmented (Lc from 74 to 50 nm)	3.5	Rotor-stator dispersion (up to 43 J/mL)	3.1.2	Heyn et al., (2021)
	Fragmented (Lc from 102 to 50 nm)		Ultra-sonication (up to 76 J mL^{-1} min^{-1})		
	SDS double layer prevents aggregation	7.0	Complexation with SDS (>1 mM) and pH adjustment to isoelectric point	4.1	Jung et al., (2008)
Semi-flexible fibrils	Unaffected	2.0	pH shift to 3.0	4.1	Mantovani et al., (2016)
	Curve into rings (500–2,000 nm diameter) and loops		Liquid-liquid interfaces (air-water & oil-water)	3.2	Jordens et al., (2014)
	Assembly of fragmented fibrils at edge of the rings				
	SDS double layer prevents aggregation		Complexation with SDS (>1 mM) and pH adjustment to isoelectric point	4.1	Jung et al., (2008)
Interfilament association	Thicker (d = 12 ± 3.1, for control d = 5.2 ± 1.1)	2.0	Complexation with SDS (>1 mM)	4.1	Jung et al., (2008)
			Complexation with maltodextrin (pH 9, 90 °C)	4.4	Karbasi et al., (2021)
	Thicker, longer pitch		Low ionic strength (undefined)	2.2	Bolisetty et al., (2011)
	Twisting filaments suppressed		High ionic strength (undefined)		
	Loss of multi-stranded fibrils (d = 2–2.5 nm, for control d = 4–10 nm)		40–50% ethanol	4.2	Jordens et al., (2011)
	Shift to worm-like aggregates (Lp from 2,369 to 29 nm)				
Aggregated and/or fragmented	Aggregated	2.0	pH shift to 5.0–7.0	4.1	Mantovani et al., (2016)
	Fragmented and aggregated		pH shift to 4.0–6.0	2.2	D. Peng et al., 2017
	Fragmented (n.d.)		pH 7.0–8.0		
	Fragmented (Lc from 290-480 nm to 80–90 nm)		Dynamic high-pressure treatment (40 MPa, three cycles)	3.1.2	Serfert et al., (2014)
	Fragmented (n.d.)		Ultrasound ($6.8*10^5$ kJ/m^3)		Mantovani et al., (2018)
	Fragmented (Lc from 7,043–107 nm)		Rotor-stator dispersion (up to 43 J/mL)		Heyn et al., (2021)
	Fragmented (Lc from 161 to 17.2 nm)		Ultra-sonication (up to 76 J/mL)		

in the presence of zinc or with specific proteases, as discussed in section 2.1), they occur with some other proteins. Generally, a higher degree of branching counteracts fibril alignment and lowers the bulk viscosity, as shown for highly branched soy protein isolate fibrils compared to slightly branched glycinin fibrils (Akkermans et al., 2007).

5.3. Networks made of stiff aggregates ($L_P > L_c$)

The post-aggregation modification of semi-flexible fibrils into smaller aggregates though mechanical treatment (section 3.1) and pH shift (section 2.1, Table 2) results in stiff and rod-like fragments if the persistence length L_p is much bigger than the contour length L_c (Storm, Pastore, MacKintosh, Lubensky, & Janmey, 2005). Thus, when semi-flexible fibrils are fragmented, L_c is reduced, but not L_p (leading to $L_p > L_c$). One can generalize that the flexibility of the fragments therefore usually decreases as a function of the size reduction, although this entails a heterogenous group of fragments varying from low flexible to rod-like.

In 1D orientation, stiff fibrils are unlikely to entangle but rather align with flow, when the concentration is high enough. The fibril concentration at which the nematic regime is reached correlates with the fibril thickness (d) and length ($\sim 1/dL^2$; Kroes-Nijboer, Venema, & Linden, 2012). Therefore, fragmented fibrils align at higher concentrations, as compared to intact fibrils. Besides, a high strength is reported for electrosprayed hierarchical fibers that are made from BLG fibrils in the presence poly (ethylene oxide), which is likely to be caused by stiff fibril elements that were produced through fracture of intact semi-flexible fibrils during the electrospraying process (Chen, Narayanan, et al., 2020; section 5.2.1). However, it could be difficult to trace the final material properties back to a particular size and flexibility.

In 2D networks stiff fibril fragments smaller than 500 nm result in reduced emulsion stability due to a decrease in viscosity in the bulk phase and incomplete surface coverage compared to semi-flexible fibrils (Mantovani et al., 2018). Different emulsion processes will affect the fibril fragment size differently and therefore the resulting emulsifying capacity will vary (section 3.1, Serfert et al., 2014).

In 2- and 3D networks, stiff fibrils form isotropic viscoelastic multilayers at surfaces and interfaces, which are disordered instead of nematic (Humblet-Hua et al., 2013). However, medium-sized rods of 100–200 nm length generated through high-pressure homogenization of semi-flexible fibrils can still have an anisotropic-nematic phase transition, albeit at approx. 10 times higher concentration than observed for semi-flexible fibrils (Jung et al., 2010). Adaption of the length of amyloid fibrils through shear stress (section 3.1) thus allows for a modulation of the phase behavior from highly elongated nematic tactoids formed with larger fibril fragments, to cholesteric droplets made from shorter fibril fragments (Bagnani, Nyström, De Michele, & Mezzenga, 2019).

6. Conclusion and outlook

This presented review and categorization provides crucial insights into the production and application of specific BLG amyloid (-like) morphologies. These can be the basis of a variety of higher order structures and networks that can be used for numerous interesting applications in materials, medicine, and food. In addition, conclusions can also be drawn as to how the morphologies change further during processing (e.g. shearing), either specifically or unintentionally.

In view of reviewing BLG fibrillization:

- Amyloid (-like) aggregates can be categorized based on their size and flexibility. Shorter and more flexible amyloid-like aggregation results from a relatively fast and less specific assembly, for example, caused by low repulsion, high concentration, or when using solvents.
- The aggregation is generally accelerated by factors that destabilize the native protein structure (e.g., high temperature, zinc, solvent, hydrolysis, interfaces, oxidation) and slows down through stabilizing factors (e.g., glycerol), or sterically hindering (e.g., protein binding with phenolic compounds or sugars).
- Mechanic post-processing (e.g., shearing, or interfacial stress) fragmentates aggregates into rods that are usually stiffer than their previous morphology.
- Chemical post-processing factors, such as addition of salts or modification with phenolic compounds (e.g. EGCG or gallic acid) can induce self-association of fibrils into tapes and sheets, while pH changes may fragment the aggregates into thinner or shorter aggregates.
- Different environmental conditions applied will affect not only the morphology-based effects but also the aggregate surface properties (i.e. surface charge and hydrophobicity). Therefore, each modification condition should be evaluated for additional chemical changes that could be beneficial for a particular application.
- When assembling into higher order structures or networks, semi-flexible morphologies can align into liquid crystalline phases or interact with linear polysaccharides (hybrid networks), while flexible aggregates have a high capacity to entangle.

The collective literature presented shows that amyloid (-like) aggregation of proteins is subject to numerous generic effects. For example, phenolic compounds prevent amyloid aggregation in both pathogenic and various food proteins. Other generic effects that accelerate the association kinetics are mechanical stress (e.g., shear and surfaces) and protein oxidation. In particular, the role of amino acid oxidation on amyloid aggregation has until now been specifically studied in pathogenic aggregation, while not much information is available for functional proteins. In addition, any safety evaluation should take various morphologies and any morphological changes caused during process modifications and digestion into account. Zhao et al. (2020) already reported the different cytotoxicity of large mature amyloids and smaller amyloid oligomers. On the whole, generic effects of natural and engineered amyloid (-like) aggregates should be further explored in the future, as this is one way to identify favorable conditions for the formation of engineered amyloid aggregates and at the same time a possibility to prevent or circumvent undesirable health effects by protein alteration.

Funding

This research is funded by the priority program SPP1934 of the German Research Foundation: DiSPBiotech – dispersity, structural and phase modifications of proteins and biological agglomerates in biotechnological processes, project number 315456892.

Author contributions

L.J.G. Hoppenreijs: conceptualization, writing – original draft, review & editing. L. Fitzner: conceptualization, writing – original draft. T. Ruhmlieb: conceptualization, writing – original draft. T.R. Heyn: conceptualization, writing – original draft. K. Schild: conceptualization, writing – original draft. A-J. van der Goot: writing – review & editing, supervision. R.M. Boom: writing – review & editing, supervision. A. Steffen-Heins: funding acquisition, conceptualization, writing – original draft, review & editing, supervision. K. Schwarz: funding acquisition, conceptualization, writing – review & editing, supervision. J.K. Keppler: project administration, funding acquisition, conceptualization, writing – original draft, review & editing, supervision.

Declaration of competing interest

None.

References

Adamcik, J., & Mezzenga, R. (2011). Adjustable twisting periodic pitch of amyloid fibrils. *Soft Matter, 7*(11), 5437–5443. https://doi.org/10.1039/c1sm05382e

Adamcik, J., & Mezzenga, R. (2018). Amyloid polymorphism in the protein folding and aggregation energy landscape. *Angewandte Chemie International Edition, 57*(28), 8370–8382. https://doi.org/10.1002/anie.201713416

Akkermans, C. (2008). *Protein fibrillization: Preparation, mechanism and application.* Wageningen University & Research.

Akkermans, C., Van Der Goot, A. J., Venema, P., Gruppen, H., Vereijken, J. M., Van Der Linden, E., et al. (2007). Micrometer-sized fibrillar protein aggregates from soy glycinin and soy protein isolate. *Journal of Agricultural and Food Chemistry, 55*(24), 9877–9882. https://doi.org/10.1021/jf0718897

Akkermans, C., van der Goot, A. J., Venema, P., van der Linden, E., & Boom, R. M. (2008). Formation of fibrillar whey protein aggregates: Influence of heat and shear treatment, and resulting rheology. *Food Hydrocolloids, 22*(7), 1315–1325. https://doi.org/10.1016/j.foodhyd.2007.07.001

Akkermans, C., Venema, P., Rogers, S. S., Van Der Goot, A. J., Boom, R. M., & Van Der Linden, E. (2006). Shear pulses nucleate fibril aggregation. *Food Biophysics, 1*(3), 144–150. https://doi.org/10.1007/s11483-006-9012-5

Akkermans, C., Venema, P., Van Der Goot, A. J., Boom, R. M., & Van Der Linden, E. (2008). Enzyme-induced formation of β-lactoglobulin fibrils by AspN endoproteinase. *Food Biophysics, 3*(4), 390–394. https://doi.org/10.1007/s11483-008-9094-3

Akkermans, C., Venema, P., van der Goot, A. J., Gruppen, H., Bakx, E. J., Boom, R. M., et al. (2008). Peptides are building blocks of heat-induced fibrillar protein aggregates of β-lactoglobulin formed at pH 2. *Biomacromolecules, 9*(5), 1474–1479. https://doi.org/10.1021/bm7014224

Al-Shabib, N. A., Khan, J. M., Malik, A., Alsenaidy, A. M., Alsenaidy, M. A., Husain, F. M., et al. (2018). Negatively charged food additive dye "Allura Red" rapidly induces SDS-soluble amyloid fibril in beta-lactoglobulin protein. *International Journal of Biological Macromolecules, 107*, 1706–1716. https://doi.org/10.1016/j.ijbiomac.2017.10.032

Al-Shabib, N. A., Khan, J. M., Malik, A., Sen, P., Alsenaidy, M. A., Husain, F. M., et al. (2019). A quercetin-based flavanoid (rutin) reverses amyloid fibrillation in β-lactoglobulin at pH 2.0 and 358 K. *Spectrochimica Acta Part A: Molecular and Biomolecular Spectroscopy, 214*, 40–48. https://doi.org/10.1016/j.saa.2019.02.004

Alavi, F., Momen, S., Emam-Djomeh, Z., Salami, M., & Moosavi-Movahedi, A. A. (2018). Radical cross-linked whey protein aggregates as building blocks of non-heated cold-set gels. *Food Hydrocolloids, 81*, 429–441. https://doi.org/10.1016/j.foodhyd.2018.03.016

Antonets, K. S., Belousov, M. V., Sulatskaya, A. I., Belousova, M. E., Kosolapova, A. O., Sulatsky, M. I., et al. (2020). Accumulation of storage proteins in plant seeds is mediated by amyloid formation. *PLoS Biology, 18*(7). https://doi.org/10.1371/journal.pbio.3000564

Arnaudov, L. N., de Vries, R., Ippel, H., & van Mierlo, C. P. M. (2003). Multiple steps during the formation of β-lactoglobulin fibrils. *Biomacromolecules, 4*(6), 1614–1622. https://doi.org/10.1021/bm034096b

Bagnani, M., Nyström, G., De Michele, C., & Mezzenga, R. (2019). Amyloid fibrils length controls shape and structure of nematic and cholesteric tactoids. *ACS Nano, 13*(1). https://doi.org/10.1021/acsnano.8b07557

Bolder, S. G., Hendrickx, H., Sagis, L. M. C., & Van Der Linden, E. (2006). Fibril assemblies in aqueous whey protein mixtures. *Journal of Agricultural and Food Chemistry, 54*(12), 4229–4234. https://doi.org/10.1021/jf060606s

Bolder, S. G., Sagis, L. M. C., Venema, P., & Van Der Linden, E. (2007). Effect of stirring and seeding on whey protein fibril formation. *Journal of Agricultural and Food Chemistry, 55*(14), 5661–5669. https://doi.org/10.1021/jf063351r

Bolder, S. G., Vasbinder, A. J., Sagis, L. M. C., & van der Linden, E. (2007). Heat-induced whey protein isolate fibrils: Conversion, hydrolysis, and disulphide bond formation. *International Dairy Journal, 17*(7), 846–853. https://doi.org/10.1016/j.idairyj.2006.10.002

Bolisetty, S., Adamcik, J., & Mezzenga, R. (2011). Snapshots of fibrillation and aggregation kinetics in multistranded amyloid β-lactoglobulin fibrils. *Soft Matter, 7*(2), 493–499. https://doi.org/10.1039/c0sm00502a

Cao, Y., & Mezzenga, R. (2019). Food protein amyloid fibrils: Origin, structure, formation, characterization, applications and health implications. *Advances in Colloid and Interface Science, 269*, 334–356. https://doi.org/10.1016/j.cis.2019.05.002

Chatani, E., Lee, Y. H., Yagi, H., Yoshimura, Y., Naiki, H., & Goto, Y. (2009). Ultrasonication-dependent production and breakdown lead to minimum-sized amyloid fibrils. *Proceedings of the National Academy of Sciences of the United States of America, 106*(27), 11119–11124. https://doi.org/10.1073/pnas.0901422106

Cheignon, C., Tomas, M., Bonnefont-Rousselot, D., Faller, P., Hureau, C., & Collin, F. (2018, April 1). Oxidative stress and the amyloid beta peptide in Alzheimer's disease. *Redox Biology*. https://doi.org/10.1016/j.redox.2017.10.014. Elsevier B.V.

Chen, D., Fang, F., Federici, E., Campanella, O., & Jones, O. G. (2020). Rheology, microstructure and phase behavior of potato starch-protein fibril mixed gel. *Carbohydrate Polymers, 239*. https://doi.org/10.1016/j.carbpol.2020.116247

Da Silva Pinto, M., Bouhallab, S., De Carvalho, A. F., Henry, G., Putaux, J. L., & Leonil, J. (2012). Glucose slows down the heat-induced aggregation of β-lactoglobulin at neutral pH. *Journal of Agricultural and Food Chemistry, 60*(1), 214–219. https://doi.org/10.1021/jf2037664

Dave, A. C., Loveday, S. M., Anema, S. G., Jameson, G. B., & Singh, H. (2014a). Glycation as a tool to probe the mechanism of β-lactoglobulin nanofibril self-assembly. *Journal of Agricultural and Food Chemistry, 62*(14), 3269–3278. https://doi.org/10.1021/jf405441g

Dave, A. C., Loveday, S. M., Anema, S. G., Jameson, G. B., & Singh, H. (2014b). Modulating β-lactoglobulin nanofibril self-assembly at pH 2 using glycerol and sorbitol. *Biomacromolecules, 15*(1), 95–103. https://doi.org/10.1021/bm401315s

Davies, M. J. (2005). The oxidative environment and protein damage. *Biochimica et Biophysica Acta (BBA) - Proteins & Proteomics, 1703*(2), 93–109. https://doi.org/10.1016/j.bbapap.2004.08.007

Davies, M. J. (2016). Protein oxidation and peroxidation. *Biochemical Journal, 473*(7), 805–825. https://doi.org/10.1042/BJ20151227

Day, L. (2013). Proteins from land plants - potential resources for human nutrition and food security. *Trends in Food Science & Technology, 32*(1), 25–42. https://doi.org/10.1016/j.tifs.2013.05.005

Deepankumar, K., Lim, C., Polte, I., Zappone, B., Labate, C., De Santo, M. P., et al. (2020). Supramolecular β-sheet suckerin–based underwater adhesives. *Advanced Functional Materials, 30*(16), 1–11. https://doi.org/10.1002/adfm.201907534

Dunstan, D. E., Hamilton-Brown, P., Asimakis, P., Ducker, W., & Bertolini, J. (2009). Shear-induced structure and mechanics of β-lactoglobulin amyloid fibrils. *Soft Matter, 5*(24), 5020–5028. https://doi.org/10.1039/b914089a

Fowler, D. M., Koulov, A. V., Balch, W. E., & Kelly, J. W. (2007). Functional amyloid - from bacteria to humans. *Trends in Biochemical Sciences, 32*(5), 217–224. https://doi.org/10.1016/j.tibs.2007.03.003

Gao, Y. Z., Xu, H. H., Ju, T. T., & Zhao, X. H. (2013). The effect of limited proteolysis by different proteases on the formation of whey protein fibrils. *Journal of Dairy Science, 96*(12), 7383–7392. https://doi.org/10.3168/jds.2013-6843

Ghadami, S. A., Khodarahmi, R., Ghobadi, S., Ghasemi, M., & Pirmoradi, S. (2011). Amyloid fibril formation by native and modified bovine β- lactoglobulins proceeds through unfolded form of proteins: A comparative study. *Biophysical Chemistry, 159*(2–3), 311–320. https://doi.org/10.1016/j.bpc.2011.08.004

Ghorbani Gorji, E., Rocchi, E., Schleining, G., Bender-Bojalil, D., Furtmüller, P. G., Piazza, L., et al. (2015). Characterization of resveratrol-milk protein interaction. *Journal of Food Engineering, 167*, 217–225. https://doi.org/10.1016/j.jfoodeng.2015.05.032

Goldschmidt, L., Teng, P. K., Riek, R., & Eisenberg, D. (2010). Identifying the amylome, proteins capable of forming amyloid-like fibrils. *Proceedings of the National Academy of Sciences of the United States of America, 107*(8), 3487–3492. https://doi.org/10.1073/pnas.0915166107

Gosal, W. S., Clark, A. H., Pudney, P. D. A., & Ross-Murphy, S. B. (2002). Novel amyloid fibrillar networks derived from a globular protein: β-Lactoglobulin. *Langmuir, 18*(19), 7174–7181. https://doi.org/10.1021/la025531a

Gosal, W. S., Clark, A. H., & Ross-Murphy, S. B. (2004). Fibrillar β-lactoglobulin gels: Part 1. Fibril formation and structure. *Biomacromolecules, 5*(6), 2408–2419. https://doi.org/10.1021/bm049659d

Gosal, W. S., Morten, I. J., Hewitt, E. W., Smith, D. A., Thomson, N. H., & Radford, S. E. (2005). Competing pathways determine fibril morphology in the self-assembly of β2-microglobulin into amyloid. *Journal of Molecular Biology, 351*(4), 850–864. https://doi.org/10.1016/j.jmb.2005.06.040

Gregersen, N., Bolund, L., & Bross, P. (2003). Protein misfolding, aggregation, and degradation 141 MOLECULAR BIOTECHNOLOGY protein misfolding, aggregation, and degradation in disease †. *Methods in Molecular Biology*. Humana Press.

Greving, I., Cai, M., Vollrath, F., & Schniepp, H. C. (2012). Shear-induced self-assembly of native silk proteins into fibrils studied by atomic force microscopy. *Biomacromolecules, 13*(3). https://doi.org/10.1021/bm201509b

Hamada, D., & Dobson, C. M. (2009). A kinetic study of β-lactoglobulin amyloid fibril formation promoted by urea. *Protein Science, 11*(10), 2417–2426. https://doi.org/10.1110/ps.0217702

Hamada, D., Tanaka, T., Tartaglia, G. G., Pawar, A., Vendruscolo, M., Kawamura, M., et al. (2009). Competition between folding, native-state dimerisation and amyloid aggregation in β-lactoglobulin. *Journal of Molecular Biology, 386*(3), 878–890. https://doi.org/10.1016/j.jmb.2008.12.038

Hamaguchi, T., Ono, K., Murase, A., & Yamada, M. (2009). Phenolic compounds prevent Alzheimer's pathology through different effects on the amyloid-β aggregation pathway. *American Journal Of Pathology, 175*(6), 2557–2565. https://doi.org/10.2353/ajpath.2009.090417

Heldt, C. L., Zhang, S., & Belfort, G. (2011). Asymmetric amyloid fibril elongation: A new perspective on a symmetric world. *Proteins: Structure, Function and Bioinformatics, 79*(1), 92–98. https://doi.org/10.1002/prot.22861

Hellwig, M. (2019). The Chemistry of protein oxidation in food. *Angewandte Chemie International Edition, 58*(47), 16742–16763. https://doi.org/10.1002/anie.201814144

Hettiarachchi, C. A., Melton, L. D., McGillivray, D. J., Loveday, S. M., Gerrard, J. A., & Williams, M. A. K. (2016). β-Lactoglobulin nanofibrils can be assembled into nanotapes via site-specific interactions with pectin. *Soft Matter, 12*(3). https://doi.org/10.1039/c5sm01530h

Heyn, T. R. (2020). *Influence of process factors on the formation and fragmentation of amyloid and amyloid-like aggregates from beta-lactoglobulin*. Kiel University.

Heyn, T. R., Garamus, V. M., Neumann, H. R., Uttinger, M. J., Guckeisen, T., Heuer, M., et al. (2019). Influence of the polydispersity of pH 2 and pH 3.5 beta-lactoglobulin amyloid fibril solutions on analytical methods. *European Polymer Journal, 120*. https://doi.org/10.1016/j.eurpolymj.2019.08.038

Heyn, T. R., Mayer, J., Neumann, H. R., Selhuber-Unkel, C., Kwade, A., Schwarz, K., et al. (2020). The threshold of amyloid aggregation of beta-lactoglobulin: Relevant factor combinations. *Journal of Food Engineering, 283*. https://doi.org/10.1016/j.jfoodeng.2020.110005

Heyn, T. R., Uttinger, M. J., Kwade, A., Peukert, W., Keppler, J. K., & Schwarz, K. (2021). Whey protein (amyloid)-aggregates in oil-water systems: The process-related comminution effect. *Journal of Food Engineering, 311*(January), 110730. https://doi.org/10.1016/j.jfoodeng.2021.110730

Humblet-Hua, N. P. K., Van Der Linden, E., & Sagis, L. M. C. (2012). Microcapsules with protein fibril reinforced shells: Effect of fibril properties on mechanical strength of the shell. *Journal of Agricultural and Food Chemistry, 60*(37), 9502–9511. https://doi.org/10.1021/jf3024529

Humblet-Hua, N. P. K., Van Der Linden, E., & Sagis, L. M. C. (2013). Surface rheological properties of liquid-liquid interfaces stabilized by protein fibrillar aggregates and protein-polysaccharide complexes. *Soft Matter, 9*(7), 2154–2165. https://doi.org/10.1039/c2sm26627j

Hu, B., Shen, Y., Adamcik, J., Fischer, P., Schneider, M., Loessner, M. J., et al. (2018). Polyphenol-binding amyloid fibrils self-assemble into reversible hydrogels with antibacterial activity. *ACS Nano, 12*(4). https://doi.org/10.1021/acsnano.7b08969

Jansens, K. J. A., Rombouts, I., Grootaert, C., Brijs, K., Van Camp, J., Van der Meeren, P., et al. (2019). Rational design of amyloid-like fibrillary structures for tailoring food protein techno-functionality and their potential health implications. *Comprehensive Reviews in Food Science and Food Safety, 18*(1), 84–105. https://doi.org/10.1111/1541-4337.12404

Jones, O. G., Handschin, S., Adamcik, J., Harnau, L., Bolisetty, S., & Mezzenga, R. (2011). Complexation of β-lactoglobulin fibrils and sulfated polysaccharides. *Biomacromolecules, 12*(8), 3056–3065. https://doi.org/10.1021/bm200686r

Jordens, S., Adamcik, J., Amar-Yuli, I., & Mezzenga, R. (2011). Disassembly and reassembly of amyloid fibrils in Water−Ethanol mixtures. *Biomacromolecules, 12*(1). https://doi.org/10.1021/bm101119t

Jordens, S., Isa, L., Usov, I., & Mezzenga, R. (2013). Non-equilibrium nature of two-dimensional isotropic and nematic coexistence in amyloid fibrils at liquid interfaces. *Nature Communications, 4*(1). https://doi.org/10.1038/ncomms2911

Jordens, S., Riley, E. E., Usov, I., Isa, L., Olmsted, P. D., & Mezzenga, R. (2014). Adsorption at liquid interfaces induces amyloid fibril bending and ring formation. *ACS Nano, 8*(11). https://doi.org/10.1021/nn504249x

Jung, J.-M. M., Gunes, D. Z., & Mezzenga, R. (2010). Interfacial activity and interfacial shear rheology of native β-lactoglobulin monomers and their heat-induced fibers. *Langmuir, 26*(19), 15366–15375. https://doi.org/10.1021/la102721m

Jung, J.-M. M., Savin, G., Pouzot, M., Schmitt, C., & Mezzenga, R. (2008). Structure of heat-induced β-lactoglobulin aggregates and their complexes with sodium-dodecyl sulfate. *Biomacromolecules, 9*(9), 2477–2486. https://doi.org/10.1021/bm800502j

Kamada, A., Mittal, N., Söderberg, L. D., Ingverud, T., Ohm, W., Roth, S. V., et al. (2017). Flow-assisted assembly of nanostructured protein microfibers. *Proceedings of the National Academy of Sciences, 114*(6). https://doi.org/10.1073/pnas.1617260114

Karbasi, M., Sánchez-Ferrer, A., Adamcik, J., Askari, G., Madadlou, A., & Mezzenga, R. (2021). Covalent β-lactoglobulin-maltodextrin amyloid fibril conjugate prepared by the Maillard reaction. *Food Chemistry, 342*(October 2020), 128388. https://doi.org/10.1016/j.foodchem.2020.128388

Kayser, J. J., Arnold, P., Steffen-Heins, A., Schwarz, K., & Keppler, J. K. (2020). Functional ethanol-induced fibrils: Influence of solvents and temperature on amyloid-like aggregation of beta-lactoglobulin. *Journal of Food Engineering, 270*(October 2019), 109764. https://doi.org/10.1016/j.jfoodeng.2019.109764

Keppler, J. K., Heyn, T. R., Meissner, P. M., Schrader, K., & Schwarz, K. (2019). Protein oxidation during temperature-induced amyloid aggregation of beta-lactoglobulin. *Food Chemistry, 289*(October 2018), 223–231. https://doi.org/10.1016/j.foodchem.2019.02.114

Khan, J. M., Qadeer, A., Chaturvedi, S. K., Ahmad, E., Rehman, S. A., Gourinath, S., et al. (2012). SDS can be utilized as an amyloid inducer: A case study on diverse proteins. *PLoS One, 7*(1). https://doi.org/10.1371/journal.pone.0029694

Knowles, T. P. J., & Mezzenga, R. (2016). Amyloid fibrils as building blocks for natural and artificial functional materials. *Advanced Materials, 28*(31), 6546–6561. https://doi.org/10.1002/adma.201505961

Knowles, T. P. J., Oppenheim, T. W., Buell, A. K., Chirgadze, D. Y., & Welland, M. E. (2010). Nanostructured films from hierarchical self-assembly of amyloidogenic proteins. *Nature Nanotechnology, 5*(3), 204–207. https://doi.org/10.1038/nnano.2010.26

Kroes-Nijboer, A., Venema, P., & Linden, E. Van Der (2012). Fibrillar structures in food. *Food and Function, 3*(3), 221–227. https://doi.org/10.1039/c1fo10163c

Lambrecht, M. A., Jansens, K. J. A., Rombouts, I., Brijs, K., Rousseau, F., Schymkowitz, J., et al. (2019). Conditions governing food protein amyloid fibril formation. Part II: Milk and legume proteins. *Comprehensive Reviews in Food Science and Food Safety, 18*, 1277–1291. https://doi.org/10.1111/1541-4337.12465

Lara, C., Adamcik, J., Jordens, S., & Mezzenga, R. (2011). General self-assembly mechanism converting hydrolyzed globular proteins into giant multistranded amyloid ribbons. *Biomacromolecules, 12*(5), 1868–1875. https://doi.org/10.1021/bm200216u

Lee, G., Lee, W., Lee, H., Lee, C. Y., Eom, K., & Kwon, T. (2015). Self-assembled amyloid fibrils with controllable conformational heterogeneity. *Scientific Reports, 5*, 1–8. https://doi.org/10.1038/srep16220

Lee, J. S., Um, E., Park, J.-K., & Park, C. B. (2008). Microfluidic self-assembly of insulin monomers into amyloid fibrils on a solid surface. *Langmuir, 24*(14). https://doi.org/10.1021/la800907c

Liu, G., Li, W., Qin, X., & Zhong, Q. (2021). Flexible protein nanofibrils fabricated in aqueous ethanol: Physical characteristics and properties of forming emulsions of conjugated linolenic acid. *Food Hydrocolloids, 114*. https://doi.org/10.1016/j.foodhyd.2020.106573

Liu, G., & Zhong, Q. (2013). Dispersible and thermal stable nanofibrils derived from glycated whey protein. *Biomacromolecules, 14*(7), 2146–2153. https://doi.org/10.1021/bm400521b

Loveday, S. M., Anema, S. G., & Singh, H. (2017). β-Lactoglobulin nanofibrils: The long and the short of it. *International Dairy Journal, 67*, 35–45. https://doi.org/10.1016/j.idairyj.2016.09.011

Loveday, S. M., & Gunning, A. P. (2018). Nanomechanics of pectin-linked β-lactoglobulin nanofibril bundles. *Biomacromolecules, 19*(7). https://doi.org/10.1021/acs.biomac.8b00408

Loveday, S. M., Su, J., Rao, M. A., Anema, S. G., & Singh, H. (2012). Whey protein nanofibrils: Kinetic, rheological and morphological effects of group IA and IIA cations. *International Dairy Journal, 26*(2), 133–140. https://doi.org/10.1016/j.idairyj.2012.03.001

Loveday, S. M., Wang, X. L., Rao, M. A., Anema, S. G., Creamer, L. K., & Singh, H. (2010). Tuning the properties of β-lactoglobulin nanofibrils with pH, NaCl and CaCl2. *International Dairy Journal, 20*(9), 571–579. https://doi.org/10.1016/j.idairyj.2010.02.014

Lux, J., Azarkh, M., Fitzner, L., Keppler, J. K. J. K., Schwarz, K., Drescher, M., et al. (2021). Amyloid aggregation of spin-labeled β-lactoglobulin. Part II: Identification of spin-labeled protein and peptide sequences after amyloid aggregation. *Food Hydrocolloids, 112*. https://doi.org/10.1016/j.foodhyd.2020.106174

MacChi, F., Hoffmann, S. V., Carlsen, M., Vad, B., Imparato, A., Rischel, C., et al. (2011). Mechanical stress affects glucagon fibrillation kinetics and fibril structure. *Langmuir, 27*(20), 12539–12549. https://doi.org/10.1021/la202125c

Maity, S., Pal, S., Sardar, S., Sepay, N., Parvej, H., Begum, S., et al. (2018). Inhibition of amyloid fibril formation of β-lactoglobulin by natural and synthetic curcuminoids. *New Journal of Chemistry, 42*(23), 19260–19271. https://doi.org/10.1039/c8nj03194k

Maity, S., Sepay, N., Pal, S., Sardar, S., Parvej, H., Pal, S., et al. (2021). Modulation of amyloid fibrillation of bovine β-lactoglobulin by selective methionine oxidation. *RSC Advances, 11*(19), 11192–11203. https://doi.org/10.1039/d0ra09060c

Makarava, N., & Baskakov, I. V. (2008). The same primary structure of the prion protein yields two distinct self-propagating states. *Journal of Biological Chemistry, 283*(23), 15988–15996. https://doi.org/10.1074/jbc.M800562200

Mantovani, R. A., de Figueiredo Furtado, G., Netto, F. M., & Cunha, R. L. (2018). Assessing the potential of whey protein fibril as emulsifier. *Journal of Food Engineering, 223*, 99–108. https://doi.org/10.1016/j.jfoodeng.2017.12.006

Mantovani, R. A., Fattori, J., Michelon, M., & Cunha, R. L. (2016). Formation and pH-stability of whey protein fibrils in the presence of lecithin. *Food Hydrocolloids, 60*, 288–298. https://doi.org/10.1016/j.foodhyd.2016.03.039

Ma, B., Zhang, F., Liu, Y., Xie, J., & Wang, X. (2018). Resveratrol induces the conversion from amyloid to amorphous aggregation of β-lactoglobulin. *Protein and Peptide Letters, 24*(12), 1113–1119.

Mohammadian, M., Salami, M., Momen, S., Alavi, F., Emam-Djomeh, Z., & Moosavi-Movahedi, A. A. (2019). Enhancing the aqueous solubility of curcumin at acidic condition through the complexation with whey protein nanofibrils. *Food Hydrocolloids, 87*(August 2018), 902–914. https://doi.org/10.1016/j.foodhyd.2018.09.001

Monge-Morera, M., Lambrecht, M. A., Deleu, L. J., Gallardo, R., Louros, N. N., De Vleeschouwer, M., et al. (2020). Processing induced changes in food proteins: Amyloid formation during boiling of hen egg white. *Biomacromolecules, 21*(6), 2218–2228. https://doi.org/10.1021/acs.biomac.0c00186

Monge-Morera, M., Lambrecht, M. A., Deleu, L. J., Louros, N. N., Rousseau, F., Schymkowitz, J., et al. (2021). Heating wheat gluten promotes the formation of amyloid-like fibrils. *ACS Omega, 6*(3), 1823–1833. https://doi.org/10.1021/acsomega.0c03670

Moores, B., Drolle, E., Attwood, S. J., Simons, J., & Leonenko, Z. (2011). Effect of surfaces on amyloid fibril formation. *PLoS One, 6*(10), 1–8. https://doi.org/10.1371/journal.pone.0025954

Munialo, C. D., Martin, A. H., Van Der Linden, E., & De Jongh, H. H. J. (2014). Fibril formation from pea protein and subsequent gel formation. *Journal of Agricultural and Food Chemistry, 62*(11), 2418–2427. https://doi.org/10.1021/jf4055215

Navarra, G., Tinti, A., Di Foggia, M., Leone, M., Militello, V., & Torreggiani, A. (2014). Metal ions modulate thermal aggregation of beta-lactoglobulin: A joint chemical and physical characterization. *Journal of Inorganic Biochemistry, 137*, 64–73. https://doi.org/10.1016/j.jinorgbio.2014.04.003

Nicoud, L., Lazzari, S., Balderas Barragán, D., & Morbidelli, M. (2015). Fragmentation of amyloid fibrils occurs in preferential positions depending on the environmental conditions. *Journal of Physical Chemistry B, 119*(13), 4644–4652. https://doi.org/10.1021/acs.jpcb.5b01160

Oboroceanu, D., Wang, L., Magner, E., & Auty, M. A. E. (2014). Fibrillization of whey proteins improves foaming capacity and foam stability at low protein concentrations. *Journal of Food Engineering, 121*. https://doi.org/10.1016/j.jfoodeng.2013.08.023

Ow, S. Y., Bekard, I., & Dunstan, D. E. (2018). Effect of natural biopolymers on amyloid fibril formation and morphology. *International Journal of Biological Macromolecules, 106*, 30–38. https://doi.org/10.1016/j.ijbiomac.2017.07.171

Peng, J., Calabrese, V., Geurtz, J., Velikov, K. P., Venema, P., & van der Linden, E. (2019). Composite gels containing whey protein fibrils and bacterial cellulose microfibrils. *Journal of Food Science, 84*(5). https://doi.org/10.1111/1750-3841.14509

Peng, D., Yang, J., Li, J., Tang, C., & Li, B. (2017). Foams stabilized by β-lactoglobulin amyloid fibrils: Effect of pH. *Journal of Agricultural and Food Chemistry, 65*(48). https://doi.org/10.1021/acs.jafc.7b03669

Petkova, A. T., Leapman, R. D., Guo, Z., Yau, W. M., Mattson, M. P., & Tycko, R. (2005). Self-propagating, molecular-level polymorphism in Alzheimer's β-amyloid fibrils. *Science, 307*(5707), 262–265. https://doi.org/10.1126/science.1105850

Porat, Y., Abramowitz, A., & Gazit, E. (2006). Inhibition of amyloid fibril formation by polyphenols: Structural similarity and aromatic interactions as a common inhibition mechanism. *Chemical Biology & Drug Design, 67*(1), 27–37. https://doi.org/10.1111/j.1747-0285.2005.00318.x

Priemel, T., Degtyar, E., Dean, M. N., & Harrington, M. J. (2017). Rapid self-assembly of complex biomolecular architectures during mussel byssus biofabrication. *Nature Communications, 8*. https://doi.org/10.1038/ncomms14539

Radovan, D., Smirnovas, V., & Winter, R. (2008). Effect of pressure on islet amyloid polypeptide aggregation: Revealing the polymorphic nature of the fibrillation process. *Biochemistry, 47*(24), 6352–6360. https://doi.org/10.1021/bi800503j

Rahaman, T., Vasiljevic, T., & Ramchandran, L. (2015). Conformational changes of β-lactoglobulin induced by shear, heat, and pH-Effects on antigenicity. *Journal of Dairy Science, 98*(7), 4255–4265. https://doi.org/10.3168/jds.2014-9010

Schleeger, M., Vandenakker, C. C., Deckert-Gaudig, T., Deckert, V., Velikov, K. P., Koenderink, G., et al. (2013). Amyloids: From molecular structure to mechanical properties. *Polymer, 54*(10), 2473–2488. https://doi.org/10.1016/j.polymer.2013.02.029

Serfert, Y., Lamprecht, C., Tan, C.-P. P., Keppler, J. K. K., Appel, E., Rossier-Miranda, F. J. J., et al. (2014). Characterisation and use of β-lactoglobulin fibrils for microencapsulation of lipophilic ingredients and oxidative stability thereof. *Journal of Food Engineering, 143*, 53–61. https://doi.org/10.1016/j.jfoodeng.2014.06.026

Shen, Y., Posavec, L., Bolisetty, S., Hilty, F. M., Nyström, G., Kohlbrecher, J., et al. (2017). Amyloid fibril systems reduce, stabilize and deliver bioavailable nanosized iron. *Nature Nanotechnology, 12*(7), 642–647. https://doi.org/10.1038/nnano.2017.58

Smith, K. B., Fernandez-Rodriguez, M.Á., Isa, L., & Mezzenga, R. (2019). Creating gradients of amyloid fibrils from the liquid–liquid interface. *Soft Matter, 15*(42). https://doi.org/10.1039/C9SM01826C

Sneideris, T., Milto, K., & Smirnovas, V. (2015). Polymorphism of amyloid-like fibrils can be defined by the concentration of seeds. *PeerJ, 2015*(8). https://doi.org/10.7717/peerj.1207

Storm, C., Pastore, J. J., MacKintosh, F. C., Lubensky, T. C., & Janmey, P. A. (2005). Nonlinear elasticity in biological gels. *Nature, 435*(7039), 191–194. https://doi.org/10.1038/nature03521

Stumpe, M. C., & Grubmüller, H. (2007). Interaction of urea with amino acids: Implications for urea-induced protein denaturation. *Journal of the American Chemical Society, 129*(51), 16126–16131. https://doi.org/10.1021/ja076216j

Usov, I., Adamcik, J., & Mezzenga, R. (2013). Serum albumin fibrils: Morphology and statistical analysis. *Faraday Discussions, 166*, 151–162. https://doi.org/10.1039/c3fd00083d

Uttinger, M. J., Heyn, T. R., Jandt, U., Wawra, S. E., Winzer, B., Keppler, J. K., et al. (2020). Measurement of length distribution of beta-lactoglobulin fibrils by multiwavelength analytical ultracentrifugation. *European Biophysics Journal, 49*(8), 745–760. https://doi.org/10.1007/s00249-020-01421-4

VandenAkker, C. C., Engel, M. F. M., Velikov, K. P., Bonn, M., & Koenderink, G. H. (2011). Morphology and persistence length of amyloid fibrils are correlated to peptide molecular structure. *Journal of the American Chemical Society, 133*(45). https://doi.org/10.1021/ja206513r

VandenAkker, C. C., Schleeger, M., Bruinen, A. L., Deckert-Gaudig, T., Velikov, K. P., Heeren, R. M. A., et al. (2016). Multimodal spectroscopic study of amyloid fibril polymorphism. *The Journal of Physical Chemistry B, 120*(34). https://doi.org/10.1021/acs.jpcb.6b05339

Veerman, C., Baptist, H., Sagis, L. M. C., & Van der Linden, E. (2003). A new multistep CA2+-induced cold gelation process for β-lactoglobulin. *Journal of Agricultural and Food Chemistry, 51*(13), 3880–3885. https://doi.org/10.1021/jf0261396

Vetri, V., & Foderà, V. (2015). The route to protein aggregate superstructures: Particulates and amyloid-like spherulites. *FEBS Letters, 589*(19), 2448–2463. https://doi.org/10.1016/j.febslet.2015.07.006

Wang, W., Nema, S., & Teagarden, D. (2010). May). Protein aggregation-Pathways and influencing factors. *International Journal of Pharmaceutics*. https://doi.org/10.1016/j.ijpharm.2010.02.025

Wei, Z., & Huang, Q. (2019). Modulation of formation, physicochemical properties, and digestion of ovotransferrin nanofibrils with covalent or non-covalent bound gallic acid. *Journal of Agricultural and Food Chemistry, 67*(35), 9907–9915. https://doi.org/10.1021/acs.jafc.9b02630

Wei, Z., & Huang, Q. (2020). Impact of covalent or non-covalent bound epigallocatechin-3-gallate (EGCG) on assembly, physicochemical characteristics and digestion of ovotransferrin fibrils. *Food Hydrocolloids, 98*(August 2019), 105314. https://doi.org/10.1016/j.foodhyd.2019.105314

Wei, G., Su, Z., Reynolds, N. P., Arosio, P., Hamley, I. W., Gazit, E., et al. (2017). Self-assembling peptide and protein amyloids: From structure to tailored function in nanotechnology. *Chemical Society Reviews, 46*(15), 4661–4708. https://doi.org/10.1039/c6cs00542j

Ye, X., Hedenqvist, M. S., Langton, M., & Lendel, C. (2018). On the role of peptide hydrolysis for fibrillation kinetics and amyloid fibril morphology. *RSC Advances, 8*(13), 6915–6924. https://doi.org/10.1039/c7ra10981d

Yoshida, K., Vogtt, K., Izaola, Z., Russina, M., Yamaguchi, T., & Bellissent-Funel, M. C. (2012). Alcohol induced structural and dynamic changes in β-lactoglobulin in

aqueous solution: A neutron scattering study. *Biochimica et Biophysica Acta (BBA) - Proteins & Proteomics, 1824*(3), 502–510. https://doi.org/10.1016/j.bbapap.2011.12.011

Zappone, B., De Santo, M. P., Labate, C., Rizzuti, B., & Guzzi, R. (2013). Catalytic activity of copper ions in the amyloid fibrillation of β-lactoglobulin. *Soft Matter, 9*(8), 2412–2419. https://doi.org/10.1039/c2sm27408f

Zhang, P., Moretti, M., Allione, M., Tian, Y., Ordonez-Loza, J., Altamura, D., et al. (2020). A droplet reactor on a super-hydrophobic surface allows control and characterization of amyloid fibril growth. *Communications Biology, 3*(1). https://doi.org/10.1038/s42003-020-01187-7

Zhang, L., & Schmit, J. D. (2017). Theory of amyloid fibril nucleation from folded proteins. *Israel Journal of Chemistry, 57*(7), 738–749. https://doi.org/10.1002/ijch.201600079

Zhao, D., Zhang, X., Xu, D., Su, G., Li, B., & Li, C. (2020). Heat-induced amyloid-like aggregation of β-lactoglobulin affected by glycation by α-dicarbonyl compounds in a model study. *Journal of the Science of Food and Agriculture, 100*(2), 607–613. https://doi.org/10.1002/jsfa.10054

Zhu, M., Souillac, P. O., Ionescu-Zanetti, C., Carter, S. A., & Fink, A. L. (2002). Surface-catalyzed amyloid fibril formation. *Journal of Biological Chemistry, 277*(52), 50914–50922. https://doi.org/10.1074/jbc.M207225200